ORNL/ENG/TM-7

Prediction of Temperature Increases in a Salt Repository Expected from the Storage of Spent Fuel or High-Level Waste

G. H. Llewellyn

ORNL/ENG/TM-7

Contract No. W-7405-eng-26

ORNL Engineering

PREDICTION OF TEMPERATURE INCREASES IN A SALT REPOSITORY EXPECTED FROM THE STORAGE OF SPENT FUEL OR HIGH-LEVEL WASTE

G. H. Llewellyn

Date Published: April 1978

OAK RIDGE NATIONAL LABORATORY
Oak Ridge, Tennessee 37830
operated by
UNION CARBIDE CORPORATION
for the
DEPARTMENT OF ENERGY

TABLE OF CONTENTS

		Page
LIST OF FIGURES		v
LIST OF TABLES		ix
FOREWORD		xi
ACKNOWLEDGMENTS		xiii
ABSTRACT		xv
1.	SUMMARY	1
2.	INTRODUCTION	3
	2.1 Background and Design Limitations	3
	2.2 Objectives of the Analysis	7
	2.3 Factors Involved in Formulating a Repository Model in Salt	7
	2.4 Definition of Temperature Terms	8
3.	SOLUTION TECHNIQUE	9
4.	HEAT SOURCES AND DECAY RATES	11
	4.1 Heat Sources Used in the Models for the Preliminary Comparisons	11
	4.2 Heat Sources Used in the Far-Field Models for the Detailed Comparisons	11
	4.3 Heat Sources Used for the Unit-Cell Models in the Detailed Comparisons	12
	4.4 Decay Rates for SF and HLW	12
	4.5 Normalized Decay Rates	15
	4.6 Ratio (SF/HLW) Stored Energy as a Function of Time	16
5.	BOUNDARY CONDITIONS	18
6.	PHYSICAL PROPERTIES AND INITIAL CONDITIONS	19
	6.1 Physical Properties	19
	6.2 Stratigraphy	19
	6.3 Initial Temperature Distribution	20
7.	PRELIMINARY COMPARISONS OF SF AND HLW AT 150 kW/ACRE AND 3.5 kW/CANISTER	23
	7.1 Two-Dimensional Far-Field Model Used in the Preliminary Comparisons — Cases A and B	25
	7.2 Two-Dimensional Unit-Cell Model Used in Preliminary Comparisons — Cases C and D	25
	7.3 Peak Temperature Increases Calculated for the Preliminary Comparisons	26

BLANK PAGE

Page

8. HEAT TRANSFER MODELS FOR DETAILED COMPARISONS OF SF STORED AT 60 kW/ACRE AND 0.55 kW/CANISTER AND HLW STORED AT 150 kW/ACRE AND 2.1 kW/CANISTER 29
   8.1 One-Dimensional Models (Cases 0 and 00) and Results 31
   8.2 Two-Dimensional Far-Field Model (Cases 1 and 2) and Numerical Results 32
   8.3 Two-Dimensional Unit-Cell Models (Cases 3 and 4) and Numerical Results 38
   8.4 Three-Dimensional Models (Cases 5 and 6) and Numerical Results 40
   8.5 Multiple Row Far-Field Model of a High-Level Waste Repository (Case 7) and Numerical Results 50

9. COMPARISON OF RESULTS FROM HIGH-LEVEL WASTE MODELS 56
   9.1 Temperature Differences as Functions of Time 56
   9.2 Temperature Increases as Functions of Depth Below the Surface of the Earth 60

10. RESULTS AND CONCLUSIONS 64

REFERENCES 66

LIST OF FIGURES

Figure		Page
2.1	Artist's conception of a radioactive waste repository . . .	5
2.2	Room spacing concept	6
4.1	Canister emplacement concept for detailed unit-cell model	13
4.2	Power production rate for PWR and BWR spent fuel assemblies and 6.28-ft^3 canisters of HLW as functions of time for periods to 100,000 years	14
4.3	Normalized heat generalized for SF and HLW as functions of time	15
4.4	Ratio (SF/HLW) of total energy released as a function of time after reprocessing or removal from reactor	17
6.1	Thermal conductivity of halite and domed salt as functions of temperature	20
6.2	Geothermal gradients	21
7.1	Midplane temperature increases in salt as functions of burial time for cases A, B, C, and D	27
7.2	Temperature increases at a depth of 2000 ft at the edge of a repository containing SF or HLW as a function of burial time	28
8.1	Peak temperature increases in one-dimensional salt models as functions of depth for SF stored at 60 kW/acre and HLW stored at 150 kW/acre	33
8.2	Two-dimensional homogenized far-field heat transfer model of a 2217-acre SF repository	34
8.3	Two-dimensional homogenized far-field heat transfer model of an 883-acre HLW repository	34
8.4	Centerline temperature increase in a two-dimensional far-field model at various times as functions of depth resulting from the storage of SF at 60 kW/acre	36
8.5	Centerline temperature increase in salt in a two-dimensional far-field model at various times as function of depth resulting from the storage of HLW at 150 kW/acre	37

Figure | Page

8.6 Midplane temperature increases in salt at various times as functions of radial distances from the centerline in a repository loaded with SF at 60 kW/acre 38

8.7 Midplane temperature increases in salt at various times as functions of radial distances from the centerline in a repository loaded with HLW at 150 kW/acre 39

8.8 Centerline temperature increase in salt in a two-dimensional far-field model at various depths as functions of time resulting from the storage of SF at 60 kW/acre 40

8.9 Centerline temperature increases in salt in a two-dimensional far-field model at various depths as functions of time resulting from the storage of HLW at 150 kW/acre 41

8.10 Midplane temperature increases at various radial locations as functions of time in a repository loaded with SF stored at 150 kW/acre 42

8.11 Midplane temperature increases at various radial locations as functions of time in a repository loaded with HLW stored at 60 kW/acre 43

8.12 Two-dimensional unit-cell model for storage of a canister containing a spent fuel assembly 44

8.13 Two-dimensional unit-cell model for storage of a canister of HLW 44

8.14 Comparison of maximum temperature increases as functions of time in the two-dimensional unit-cell models for SF stored at 60 kW/acre and HLW stored at 150 kW/acre 45

8.15 Three-dimensional unit-cell model for a PWR spent fuel assembly or HLW canister 46

8.16 Comparison of maximum temperature increases in salt as functions of time in the three-dimensional unit-cell models for SF stored at 60 kW/acre and HLW stored at 150 kW/acre 47

Figure		Page
8.17	Comparison of maximum temperature on the floor of the storage room as functions of time due to SF stored at 60 kW/acre and HLW stored at 150 kW/acre	48
8.18	Contours for temperature increases in the *XZ* plane 25 years after burial in the three-dimensional unit-cell model for SF stored at 60 kW/acre	49
8.19	Contours for temperature increases in the horizontal midplane 25 years after burial in the three-dimensional unit-cell model for SF stored at 60 kW/acre	50
8.20	Contours for temperature increases in the *XZ* plane 5 years after burial in the three-dimensional unit-cell model for HLW stored at 150 kW/acre	51
8.21	Contors for temperature increases in the horizontal midplane 5 years after burial in the three-dimensional unit-cell model for HLW stored at 150 kW/acre	52
8.22	Section through multiple row model showing repository from the center to the edge	53
8.23	Temperature increases at various depths in the salt repository as a function of horizontal position	54
9.1	Comparison of temperature increases from various models of an HLW repository as functions of time	57
9.2	Comparison of midplane temperature increases on outer edge of repository obtained from two-dimensional far-field models storing HLW at 150 kW/acre as functions of time	60
9.3	Midplane temperature increases in far-field models produced by SF and HLW as a function of areal heat load	61
9.4	Comparison of peak temperature increases obtained from various far-field models for storing HLW as functions of depth below the surface of the earth	62
9.5	Comparison of peak temperature increases from two- and three-dimensional unit-cell models as functions of depth below the surface of the earth, incurred in the storage of HLW at 150 kW/acre	63

LIST OF TABLES

Table		Page
2.1	Radioactive waste types considered in repository design	4
7.1	Two-dimensional R,Z computer models for preliminary comparisons — cases A through D	24
8.1	Computer models for detailed comparisons — cases 0 through 7	30

FOREWORD

This report was prepared by the Engineering Division of Union Carbide Corporation, Nuclear Division, in cooperation with the Office of Waste Isolation and is part of the National Waste Terminal Storage Program. The principal objective of this program is to establish facilities in various deep geologic formations at several locations in the United States which will safely dispose of commercial radioactive waste. This report considers the waste to be either unreprocessed spent fuel or high-level waste. As part of the Thermal Analysis Studies of the Office of Waste Isolation, this report compares the thermal responses to the burial of spent fuel and high-level waste in hypothetical repositories in salt.

ACKNOWLEDGMENTS

The author wishes to acknowledge the help of W. A. Burnett of OWI and M. Siman-Tov of UCC-ND Engineering Division in the organization and review of the report and W. D. Turner and D. C. Elrod, of UCC-ND Computer Sciences Division, for their assistance in processing and verification of the computer models. Appreciation is extended to T. Whitus, J. M. Hackworth, J. R. McIntosh, and R. D. Harrell for the figures used in the report. This report was sponsored by the Office of Waste Isolation, UCC-ND, Oak Ridge, Tennessee.

ABSTRACT

Comparisons in temperature increases incurred from hypothetical storage of 133 MW of 10-year-old spent fuel (SF) or high-level waste (HLW) in underground salt formations have been made using the HEATING5 computer code. The comparisons are based on far-field homogenized models that cover areas of 65 and 25 sq miles for SF and HLW, respectively, and near-field unit-cell models covering respective areas of 610 ft^2 and 400 ft^2. Preliminary comparisons based on heat loads of 150 kW/acre and 3.5 kW/canister indicated near-field temperature increases about 20% higher for the storage of the spent fuel than for the high-level waste. In these comparisons, it was also found that the thermal energy deposited in the salt after 500 years is about twice the energy deposited by the high-level waste.

The thermal load in a repository containing 10-year-old spent fuel was thus limited to 60 kW/acre to obtain comparable far-field thermal effects as obtained in a repository containing 10-year-old high-level waste loaded at 150 kW/acre. Detailed far-field and unit-cell comparisons of transient temperature increases have been made based on these loadings. Unit-cell comparisons were made between a canister containing high-level waste with an initial heat production rate of 2.1 kW and a canister containing a PWR spent fuel assembly producing 0.55 kW.

Using a three-dimensional unit-cell model, a maximum salt temperature increase of 260°F was calculated for the high-level waste prior to backfilling (5 years after burial), whereas a maximum temperature increase of 110°F was calculated for the spent fuel prior to backfilling (25 years after burial).

Comparisons were also made between various configurational models for the high-level waste showing the applicability of each model.

1. SUMMARY

Preliminary comparisons have been made between the thermal responses of high-level waste (HLW) and spent fuel assemblies (SF), each stored in salt repositories at an areal heat load of 150 kW/acre and an initial canister heat production rate of 3.5 kW. The results of these studies, based on unit-cell models, indicate a maximum peak temperature increase of 337°F in the salt for the SF storage — about 12% higher than the peak temperature increase predicted for the HLW. The temperature increases based on far-field models were found to be practically uniform throughout most of the repository. The SF repository temperature increase peaked at 253°F, which is about 18% higher than the increase calculated for the HLW.

A thermoelastic analysis[1] based on far-field models showed that SF stored at 60 kW/acre produces an upheaval of about 54 in. after 1000 years, which is comparable to the upheaval calculated for HLW loaded at 150 kW/acre. Therefore, additional analyses were performed to compare temperature distributions resulting from the storage of 10-year-old SF at an areal heat load of 60 kW/acre and 0.55 kW/canister with those based on the storage of HLW at 150 kW/acre and 2.1 kW/canister. In an effort to obtain more accurate localized temperatures for the actual canister emplacement, three-dimensional unit-cell models were created. The analyses made on the three-dimensional unit-cell model containing SF indicated that a maximum temperature increase (ΔT) of 105°F is reached in the salt prior to backfilling (25 years after burial), and a peak maximum ΔT of 113°F is reached after 35 years. A peak maximum temperature increase of 105°F reached after 60 years was found in the two-dimensional unit-cell model. The detailed analyses of the HLW storage indicate maximum ΔTs of 260°F for the three-dimensional unit-cell model after 5 years (which is the proposed backfilling time) with a peak maximum ΔT of 301°F reached in about 20 years. A peak maximum ΔT of 269°F reached in about 25 years was found in the two-dimensional unit-cell model.

The results of all of the unit-cell models were compared with the interim thermal criteria,[2] which allows 1% of the salt in a unit cell to exceed 482°F and 25% to exceed 392°F. It was found that these specific thermal criteria are completely satisfied.

BLANK PAGE

The far-field analysis indicated a fairly uniform temperature throughout the repository midplane; the temperature peaked at about 100°F 60 years after burial for SF and at about 225°F 35 years after burial for HLW.

Although the peak temperature increases were about twice as great for HLW as for SF, the total energy delivered to the salt is about the same, resulting in comparable upheavals in both cases.

2. INTRODUCTION

2.1 Background and Design Limitations

The Department of Energy is currently considering whether or not permanent disposal of radioactive waste can be effectively accomplished by burying it in geological formations in a concentrated solid form. Solid radioactive wastes, which are produced in various types as shown in Table 2.1,[3] include spent fuel, high-level waste, cladding waste, intermediate-level transuranic waste, and low-level transuranic waste. The maximum heat generation rates were evaluated from available data and are included in Table 2.1 for comparison. The SF contains only products that result from spent UO_2.

Internal heat generation produced by the decay of the radioactive wastes can present major thermal problems, and consequently the amount that can be stored safely in a specified area of a given medium is limited. High-level waste and spent fuel are the major causes of concern because they have much higher rates of heat production than the other waste forms. Many geological formations are under consideration by the National Waste Terminal Storage (NWTS) program for the establishment of federal repositories. Dome salt, bedded salt, shale, and granite are currently being investigated as potential storage media. The Office of Waste Isolation (OWI) is currently in the process of formulating conceptual designs for repositories in salt formations. An artist's conception of a repository in bedded salt is shown in Fig. 2.1. The storage area is located in rooms excavated about one-half mile below the surface of the earth. The waste is stored in canisters placed in holes drilled along the centerline of the room. Figure 2.2 illustrates the storage configuration that is used in this report with 18-ft square rooms and 60-ft pillars. It should be pointed out that other configurations could be used in repository design. Up to 5.3 kW/canister of HLW has been previously considered and analyzed for storage in a salt repository by Cheverton and Turner.[4] The HLW can be stored in calcine, glass, ceramics, or matrix metal. At present one of the most promising forms of containment material is borosilicate glass, which is relatively

Table 2.1. Radioactive waste types considered in repository design

Spent fuel assemblies (heat generation less than 28,000 W/m^3)

Pressurized-water reactor (PWR) spent fuel assemblies are assumed to be fueled with 3.3% enriched (^{235}U) and subjected to an exposure of 33,000 MWd/MTU (1100 days at an average specific power of 30 MW/MT). The mass of uranium per assembly is 0.4614 MT.

Boiling-water reactor assemblies are assumed to be subjected to an exposure of 27,500 MWd/MTU (1328.5 days at an average specific power of 20.7 MW/MTU). The mass of uranium per assembly is 0.1833 MT.

High-level waste (heat generation less than 28,000 W/m^3)

Solidified composites of all the liquid waste streams arising from the reprocessing of spent fuels. These wastes contain more than 99.9% of the nonvolatile fission products, 0.5% of the uranium and plutonium, and all the other actinides formed by transmutation of the uranium and plutonium in the reactor.

Cladding waste (heat generation less than 400 W/m^3)

Solid fragment of zircaloy and stainless steel cladding and other structural components of the fuel assemblies that remain after the fuel cores have been dissolved. These fragments are compacted to 70% of theoretical density. In addition to neutron-induced radioactivity, the cladding waste contains 0.05% of the actinides and 0.05% of the nonvolatile fission products in the spent fuel.

Intermediate-level transuranic waste (heat generation less than 1.9 W/m^3)

Those solids or solidified materials (other than high-level and cladding wastes) that contain long-lived alpha emitters at concentrations greater than 10 n/Ci/g, and have typical surface dose rates between 10 and 1000 millirems/hr after packaging due to fission-product contamination.

Low-level transuranic waste (heat generation less than 1.2 W/m^3)

Those solids or solidified materials that contain plutonium or other long-lived alpha emitters in known or suspected concentrations greater than 10 n/Ci/g, and yet have sufficiently low external radiation levels after packaging that they can be handled directly

ORNL-DWG 76-20534

Fig. 2.1. Artist's conception of a radioactive waste repository.

ORNL-DWG 78-5466

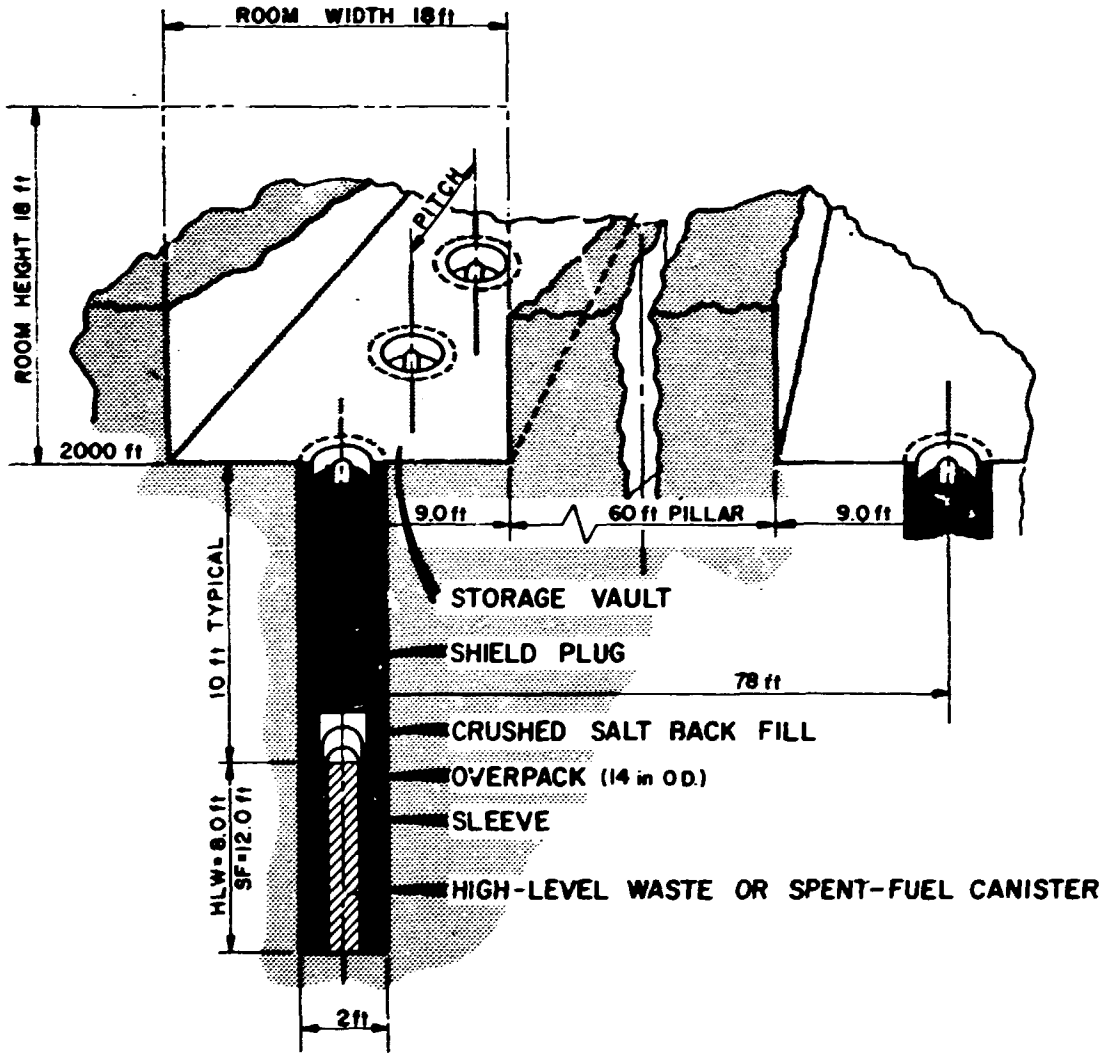

Fig. 2.2. Room spacing concept.

inexpensive and has a high devitrification temperature. The SF can also be encapsulated in different ways.

The heat produced by the buried waste is dissipated into the surrounding medium by conduction and is finally transferred from the earth's surface to the atmosphere by natural convection and eventually to deep space by thermal radiation. During this process, a peak temperature is reached in the repository close to the centroid of the heat source. After reaching a maximum value, this peak temperature decreases as a function of time due to the decay of the radioactive materials contained in the canisters.

Repository design involves detailed heat transfer and rock mechanics studies, including stress and deformation analyses. Temperatures in a salt repository must be controlled because the heat produced by the waste causes an increase in creep rate leading to accelerated room closure. After backfilling a room with crushed salt, this consideration is of less importance. It is also necessary to control the temperature to limit the surficial uplift due to thermal expansion, which might compromise the integrity of the repository and/or its environment.

Heat transfer and material evaluations inside of the canister itself are important factors in limiting the heat loads used in the repository, but these points are being considered in other studies.

2.2 Objectives of the Analysis

The purpose of these heat transfer analyses is to provide temperature distributions to be used in structural, safety, and environmental evaluations to confirm the structural integrity in conceptual repository design. The objectives of these analyses are (1) to determine from the transient temperature distributions when and where the peak temperatures occur, (2) to compare the temperature rises obtained from the storage of SF and HLW, and (3) to compare the results obtained from the various models employed. Thermal effects in the repository medium are the main concern, and only temperatures in the medium are considered relevant in this study.

2.3 Factors Involved in Formulating a Repository Model in Salt

In order to attain these objectives, models must be created to simulate as accurately and economically as possible the actual situation that will be encountered when large amounts of heat (up to 133 MW) in the form of radioactive wastes are buried in a repository. This burial can be in the terminal mode where the excavated rooms are backfilled with crushed salt, or it can be in a retrievable mode where the rooms are left open to provide the capability of access to or removal of the canisters during the retrievability period. Backfilling may occur as soon as 5 years after

burial for the HLW or as long as 25 years for the SF under the present conceptual design for deep geological disposal. The most important factors in the thermal analysis of repository models are (1) the initial heat production rate, the distribution, and decay rate of the radioactive waste material, (2) the stratigraphy of the repository, (3) thermal and physical properties of the storage medium, and (4) boundary conditions including the geothermal flux and the dimensions of the models. The dimensions of the models should be within the range of temperature propagation. The question of using isothermal or adiabatic boundaries was resolved by using economical one-dimensional solutions in parametric studies. Use of these studies was found to be less costly to establish the boundary limits.

The selection and proper use of these factors in relation to models considered will be discussed in later sections.

2.4 Definition of Temperature Terms

In general the meaning of the temperature terms referred to in this report are as follows.

1. ΔT or temperature increase refers to localized temperature increase above a steady-state initial temperature of a given position.
2. Maximum ΔT or maximum temperature increase is the highest ΔT with respect to position at any given time.
3. Peak ΔT or peak temperature increase is the highest ΔT with respect to time at a given position.
4. Peak maximum ΔT or peak maximum temperature increase is the highest ΔT with respect to time reached at a given location which also has the highest ΔT with respect to position.

3. SOLUTION TECHNIQUE

The problem at hand is to determine the transient temperature distributions resulting from a finite decaying heat source in a multiregion finite media for which the thermal diffusivities are moderate functions of temperatures. As long as the boundary conditions and thermal properties are considered to be constant, analytical solutions can be considered. Carslaw and Jaeger[5] have presented basic formulations that have been expanded to geological applications by Ingersoll et al.[6] J. P. Nichols[7] of ORNL developed several unique analytical solutions for conduction in an infinite medium with a decaying heat source by employing Green's function and the method of both superposition and the assumption of instantaneous heat release.

Although analytical solutions can provide insight with respect to physical mechanisms, numerical techniques must be employed to incorporate the nonlinearities caused by temperature-dependent thermal properties and boundary conditions in a multicomponent medium.

Many general-purpose finite difference and finite element programs are available for the solution of the nonlinear conduction problems. TRUMP,[8] AYER,[9] and NOHEAT[10] were several of the finite element codes considered and offered no apparent advantage over HEATING5,[11] which was used for these investigations.

HEATING5, the latest modification in a series of HEATING programs, is a general finite difference heat transfer program for both steady-state and transient heat transfer problems in one-, two-, or three-dimensional configurations. All thermal transport properties can be expressed as functions of temperature, and nonlinear boundary conditons can be imposed. Heat generation can be expressed as a function of time and position. The boundary conditions can be specified as adiabatic, forced convection, natural convection, radiation, constant temperature, or constant heat flux. The boundary conditions can be temperature and/or time dependent.

Both explicit and implicit techniques are available for the solution of transient heat transfer problems. The implicit techniques include the Classical Implicit Procedures (CIP), backwards Euler, or Crank-Nicholson.

The Crank-Nicholson[12] implicit solution technique was chosen for the transient analyses in these investigations, using an initial time-step of 0.1 year. Cheverton and Turner[13] give an excellent discussion on various solution techniques, including their assets, liabilities, and economics.

The HEATING5 code has been modified to remove the limits on the size of the arrays used in the input variables and to reduce the core requirements for a given problem. This modified version is designated as HEATING5A,[14] which was used to analyze problems that could not be processed using HEATING5. TRUMP was compared[15] with HEATING5 and was found to require as much as 100 times the CPU time required to obtain steady-state solutions and as much as 2.5 times the CPU time required to obtain transient solutions on nonlinear problems as was required using HEATING5.

The HEATING programs used at the Union Carbide Corporation installations at Oak Ridge for the past 14 years have been found to be accurate, versatile, and dependable and have proved to be beneficial in obtaining solutions in many types of complex heat transfer problems.

4. HEAT SOURCES AND DECAY RATES

It is assumed that the hypothetical repository used in this study should have the capability of storing 133 MW of 10-year-old SF or HLW by the year 2010, which is close to the 121 MW projected by Kee, Croff, and Blomeke.[16] The canisters are conservatively assumed to be uniformly and simultaneously loaded in the repository for determination of the heat generation rate of the far-field source. For an 80-ft room spacing with a canister pitch of 80 ft and a heat load of 160 kW/acre, Cheverton and Turner[17] calculated a maximum temperature rise about 10°F greater for simultaneous loading than for sequential loading of a repository.

4.1 Heat Sources Used in the Models for the Preliminary Comparisons

The far-field heat source for the two-dimensional R,Z models used in the preliminary comparisons is obtained by distributing the 133 MW of heat uniformly throughout the repository volume. The 883-acre repository area is determined by distributing the far-field heat source of 133 MW at 150 kW/acre. The height of the source is assumed to be 10 ft in the preliminary models, yielding a volume of 3.85×10^8 ft^3 and an initial heat generation rate of 10,353 Btu/yr·ft^3 for the 10-year-old source. This initial source strength is used for both SF and HLW in the preliminary models.

The unit-cell heat source for the preliminary models for both SF and HLW is based on an initial heat load of 3.50 kW/canister for 10-year-old waste. The 10-year-old waste in the unit cell is assumed to have a diameter of 16 in. and a height of 10 ft, yielding a volume of 13.96 ft^3 and an initial heat generation rate of 7.49×10^5 Btu/yr·ft^3.

4.2 Heat Sources Used in the Far-Field Models for the Detailed Comparisons

The far-field heat source for the models used in the more detailed analyses is obtained by uniformly distributing the 133 MW of heat from

the 10-year-old waste over the cylindrical source volumes of the models. The volume occupied by the source for the SF model has a radius of 5544 ft (based on an areal heat load of 60 kW/acre) and a height of 12 ft (the active height of a fuel assembly). The resulting homogenized heat generation rate is 3432 Btu/yr·ft^3 for 10-year-old SF.

In like manner, the volume of the far-field heat source of HLW has a 3500-ft radius (based on an areal heat load of 150 kW/acre) and a height of 8 ft (the active height of HLW in the canister). The resulting homogenized heat generation rate for 10-year-old HLW is 12,916 Btu/yr·ft^3.

4.3 Heat Sources Used for the Unit-Cell Models in the Detailed Comparisons

The heat source used in the unit-cell model for SF is assumed to be a spent pressurized water reactor (PWR) fuel assembly that has been removed from the reactor for 10 years and has a power of 0.55 kW. The source strength of 10-year-old HLW is 2.1 kW. This heat was distributed over separate volumes for the SF and HLW.

The volume of the unit-cell sources for the detailed comparisons as shown in Fig. 4.1 is based on a diameter of 20 in. The height of the source used for the SF is 12 ft, resulting in a volumetric heat generation rate of 6.27×10^5 Btu/yr·ft^3. The active height of the HLW is 8.0 ft, resulting in a heat generation rate of 3.70×10^6 Btu/yr·ft^3. The assumption made in these cases is that the crushed salt used as backfill recrystallizes into the solid form in a relatively short time so that the backfill properties can be assumed to be the same as those of solid salt.

4.4 Decay Rates for SF and HLW

The SF may be in the form of fuel element assemblies from either a pressurized water reactor (PWR) or a boiling water reactor (BWR). In this study, the SF is assumed to be from PWRs because of the slower decay of their heat generation rate, but the power production rates for the BWR assemblies will be shown for comparison. The power production rates in

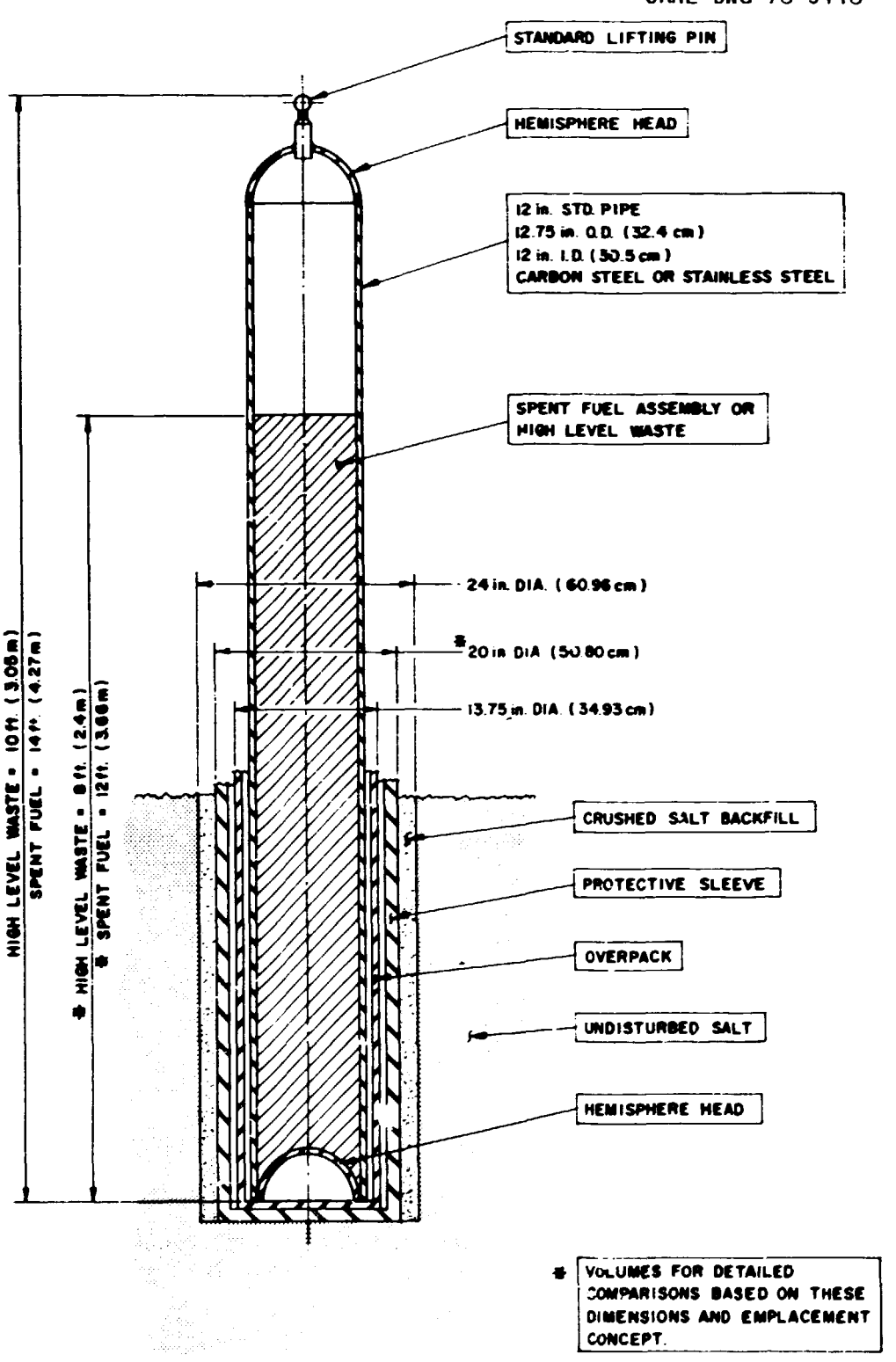

Fig. 4.1. Canister emplacement concept for detailed unit-cell model.

kilowatts are shown in Fig. 4.2 for SF assemblies and HLW canisters as functions of time after reprocessing or discharge from a reactor over a period of 100,000 years.

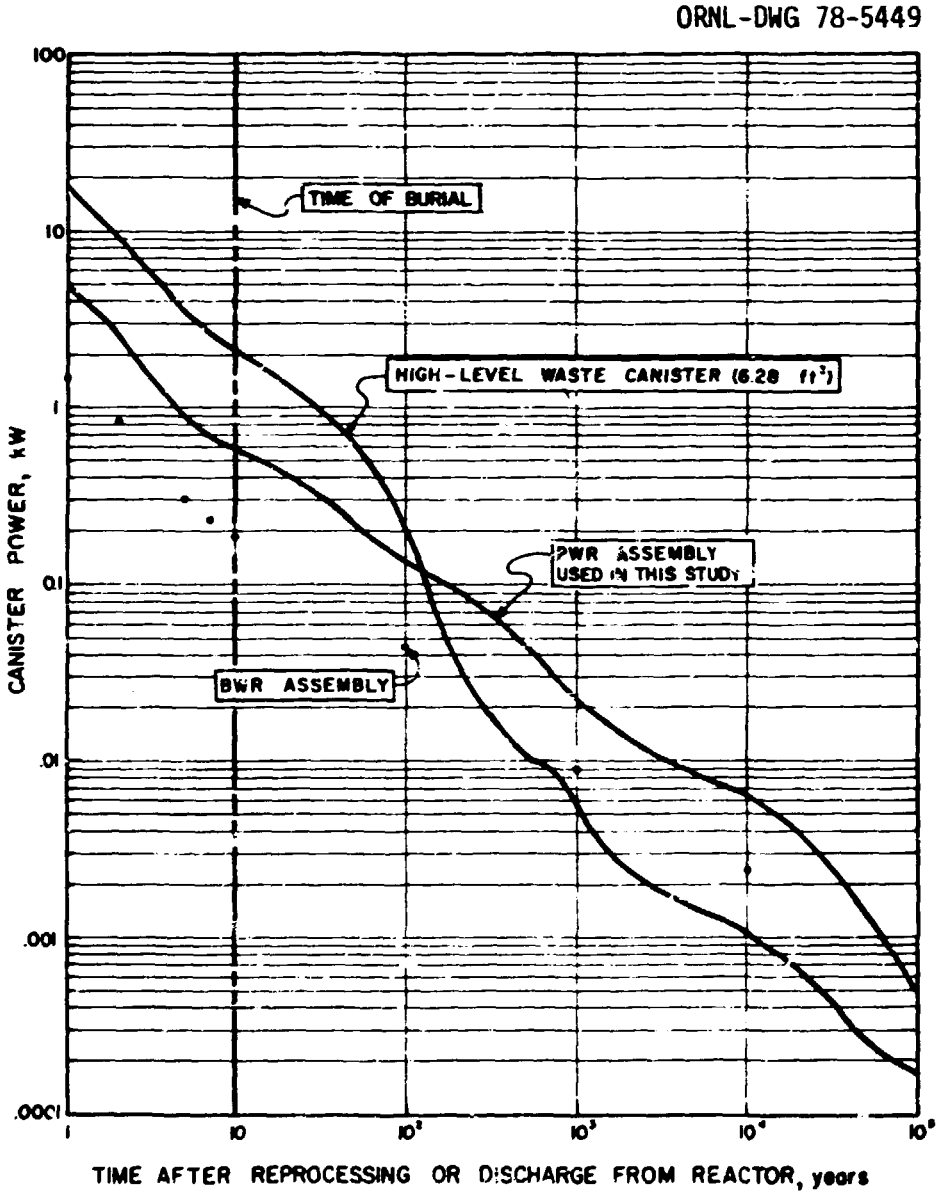

Fig. 4.2. Power production rate for PWR and BWR spent fuel assemblies and 6.28-ft^3 canisters for HLW as functions of time for periods to 100,000 years.

4.5 Normalized Decay Rates

The heat generation rates of PWR and BWR spent fuel assemblies and HLW were obtained through the use of the ORIGEN[18] computer program as a function of time over a period of 100,000 years. To obtain a dimensionless relationship that can be used to evaluate any given source as a function of time, the data were normalized by dividing the time-dependent heat generation rates by their respective initial values at 1 year. The HLW was also assumed to be aged 160 days prior to processing. The normalized heat generation rates for both SF and HLW are shown in Fig. 4.3.

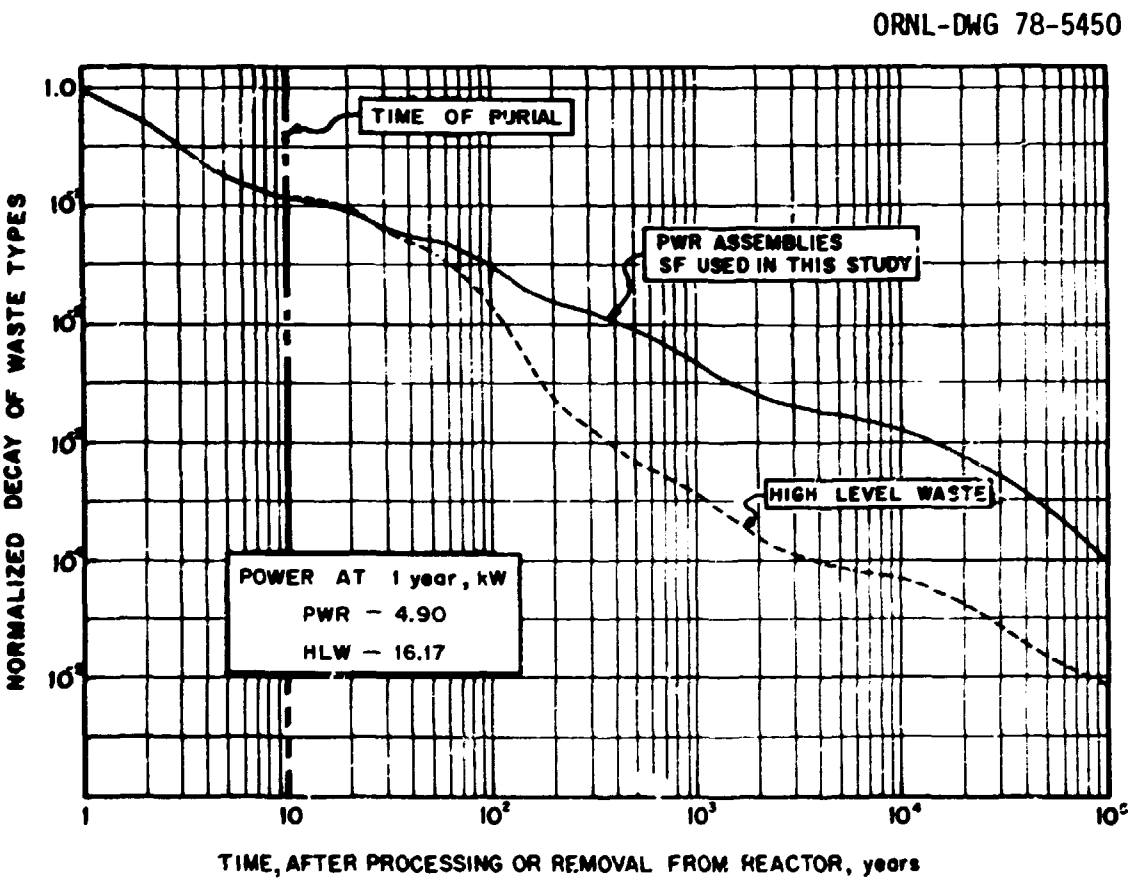

Fig. 4.3. Normalized heat generalized for SF and HLW as functions of time.

During the first 20 years, very little difference exists between the two curves, but the difference steadily increases with time to a point at which the SF is producing heat at a rate as much as 20 times as great as the HLW. The dominating factor in the heat decay is the presence of ^{239}Pu, which has a half-life of 24,000 years. The HLW contains only 0.5% as much plutonium as the SF.

4.6 Ratio (SF/HLW) Stored Energy as a Function of Time

It is interesting to compare the integrated power, or energy, of an initially equal power source of HLW and SF as a function of time. The energy for each waste type was obtained by integrating the power as a function of time based on tabulation of the ORIGEN output data for reprocessed HLW and PWR spent fuel assemblies. The ratio (SF/HLW) was obtained by dividing the normalized value obtained for SF by the normalized value obtained for HLW. This ratio (SF/HLW) of energy released as a function of time is shown in Fig. 4.4 This difference between SF and HLW is due to the higher ^{239}Pu content of the SF.

The difference in the upheavals in SF and HLW repositories with the same areal heat loads is primarily due to the stored energy. Thus by reducing the areal heat load of the SF from 150 kW/acre to 60 kW/acre, the upheaval was made about equal to that incurred by the HLW stored at 150 kW/acre.

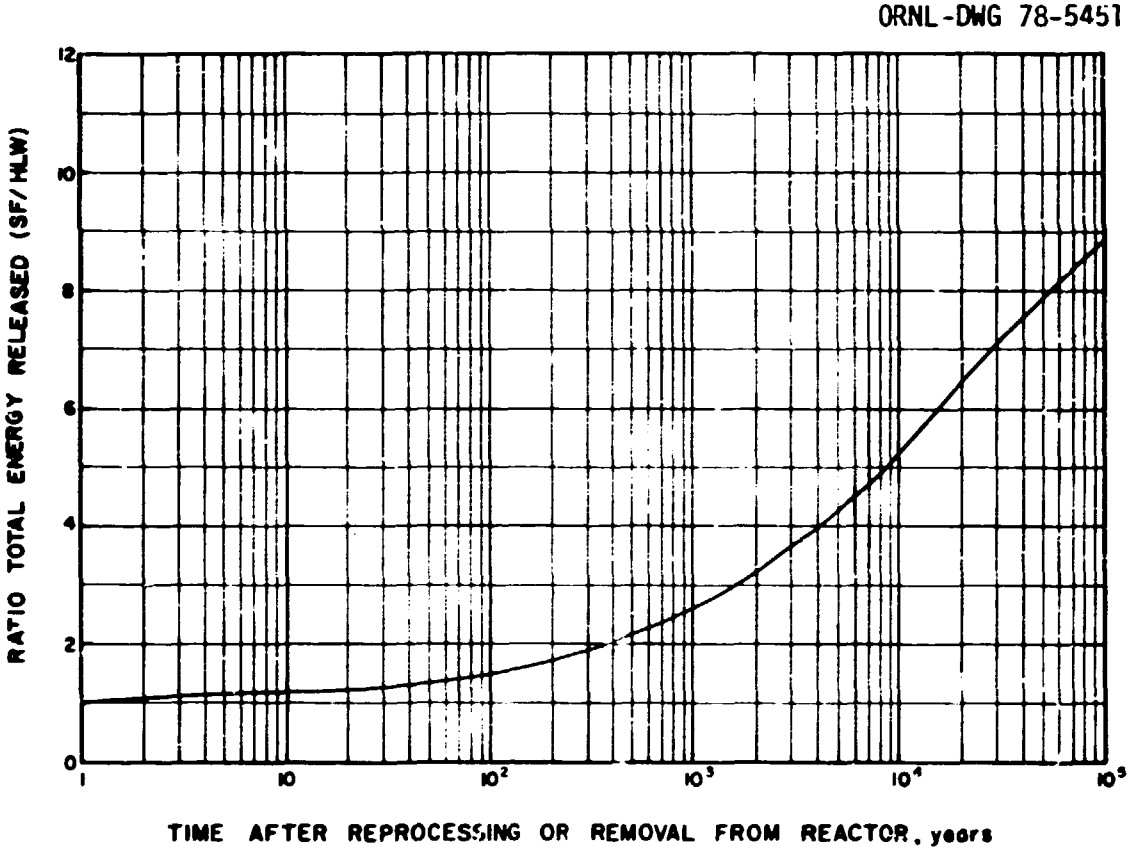

Fig. 4.4. Ratio (SF/HLW) of total energy released as a function of time after reprocessing or removal from reactor.

5. BOUNDARY CONDITIONS

Boundary conditions required for the heat transfer models used in these investigations are the surface-air temperature, heat transfer coefficient at the surface, and the prevailing geothermal flux. Diurnal and seasonal perturbations in the bulk air temperature over the repository are not important in this analysis because these perturbations disappear at depths below 50 ft.[19] Consequently, a constant surface-air temperature of 60°F has been assumed in these analyses, which is close to the mean annual temperature found in the United States.

To evaluate the magnitude of the temperature difference on the surface, the heat transfer coefficient must be considered. This coefficient is a function of such factors as local terrain, ground conditions, and the temperature and velocity of the air; the mean value generally varies between 2 and 6 Btu/hr·ft^2·°F.[20] A mean value of 4.0 Btu/hr·ft^2·°F was used in these analyses.

Geothermal fluxes in the continental United States[21] usually range from 53 to 350 Btu/yr·ft^2. A mean geothermal flux of 140 Btu/yr·ft^2 has been estimted for the land masses and was imposed on the lower axial boundary of all heat transfer models used in this report.[22]

Using a mean surface heat transfer coefficient of 4 Btu/hr·ft^2·°F, a ΔT of only 0.004°F is required to dissipate the geothermal flux to the air by forced convection. A maximum surface ΔT of 0.01°F was calculated in these analyses as required to transfer the heat load by forced convection to the air. This is only about 2-1/2 times the ΔT produced by the mean geothermal flux.

Adiabatic conditions have been assumed on the radial boundaries of all of the heat transfer models. In far-field parametric studies made on the two-dimensional models for HLW and SF, the radial boundary extended to 15,000 ft and 24,000 ft respectively. No appreciable increase was noted in the initial boundary temperatures after reaching the final time of 100,000 years.

6. PHYSICAL PROPERTIES AND INITIAL CONDITIONS

6.1 Physical Properties

The physical property data used in these calculations are the same as those used by Cheverton and Turner[23] with the exception of the overburden material. The overburden that was assumed has constant physical properties with a thermal conductivity of 1.0 Btu/hr·ft·°F, a density of 150 lb/ft^3, and a heat capacity of 0.20 Btu/lb·°F. The shale strata existing in the detailed far-field models below a depth of 4000 ft is also assumed to have constant physical properties identical with those listed for the overburden material.

The salt formation is assumed to be halite, which is essentially pure sodium chloride. The heat capacity and density of halite change very little over the temperature range 50 to 500°F. The heat capacitance of halite is assumed to be constant at 0.22 Btu/lb·°F and the density constant at 135 lb/ft^3. The thermal conductivity of halite used in this report is from data of Birch and Clarke,[24] who obtained values of 3.53 Btu/hr·ft·°F at 32°F to 1.20 Btu/hr·ft·°F at 732°F. Thermal conductivities for domed salt were obtained for temperatures up to 1200°F by Smith,[25] who employed a newly developed laser technique. The data obtained by Smith are included for comparison in Fig. 6.1, along with the data obtained by Birch and Clarke.

6.2 Stratigraphy

The stratigraphy for an actual repository naturally will be site dependent and variable in both horizontal and vertical directions. The stratigraphy employed in this study is hypothetical, and certain simplifying assumptions have been made for the purpose of modeling the repository.

The model overburden used in the preliminary investigations was assumed to extent to a depth of 800 ft, with halite extending below this point to a depth of 24,000 ft. The thermal conductivity of the halite is assumed to be a function of temperature.

The stratigraphy assumed for the detailed far-field models assumes a constant physical property overburden to a depth of 800 ft. A strata

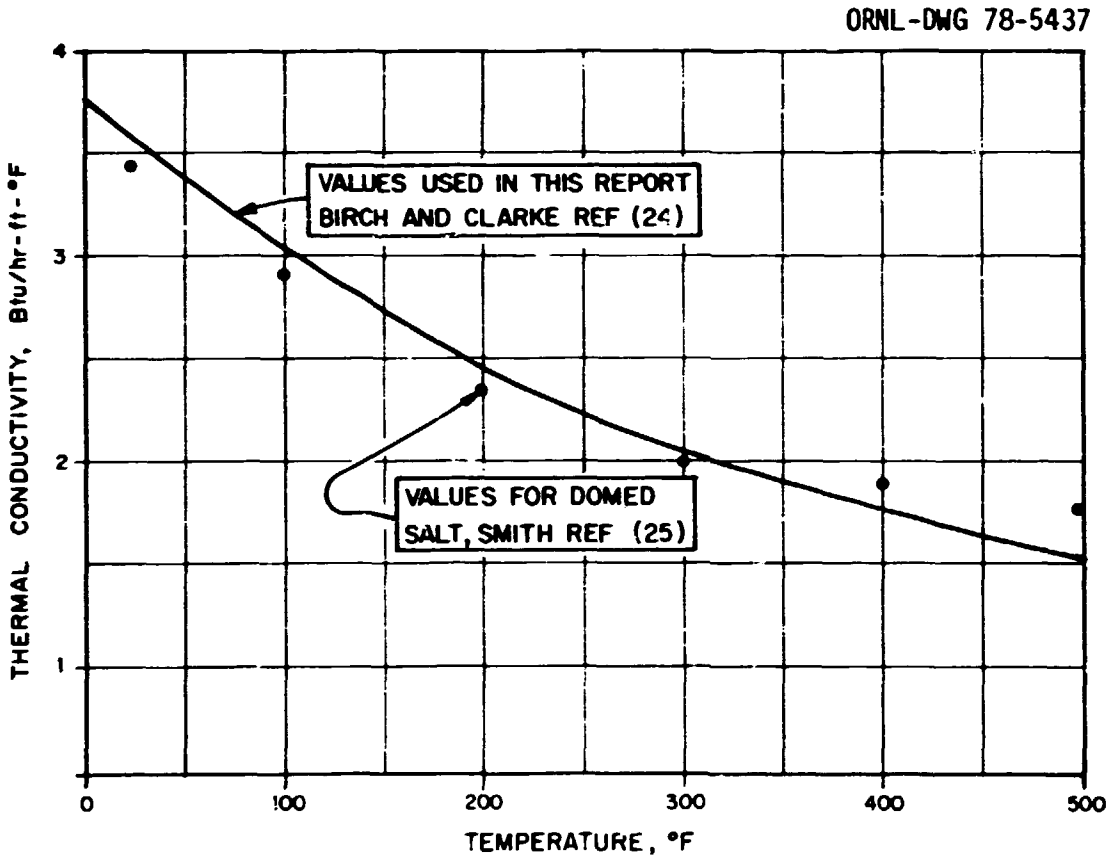

Fig. 6.1. Thermal conductivity of halite and domed salt as functions of temperature.

of halite is assumed from 800 ft to a depth of 4000 ft. Shale is assumed to exist from the 4000-ft elevation downward to the 24,000-ft elevation.

The stratigraphy is an important factor in establishing an initial geothermal gradient as will be discussed in Sect. 6.3. When actual repository sites have been identified, finer definition of the stratigraphy can be made.

6.3 Initial Temperature Distribution

The geothermal flux and thermal conductivity were used to obtain initial temperature distributions from a one-dimensional steady-state heat transfer model based on the assumed stratigraphies of the far-field models as mentioned in Sect. 6.2. The resulting initial thermal gradients used in the models are shown in Fig. 6.2. Nonlinear gradients are encountered

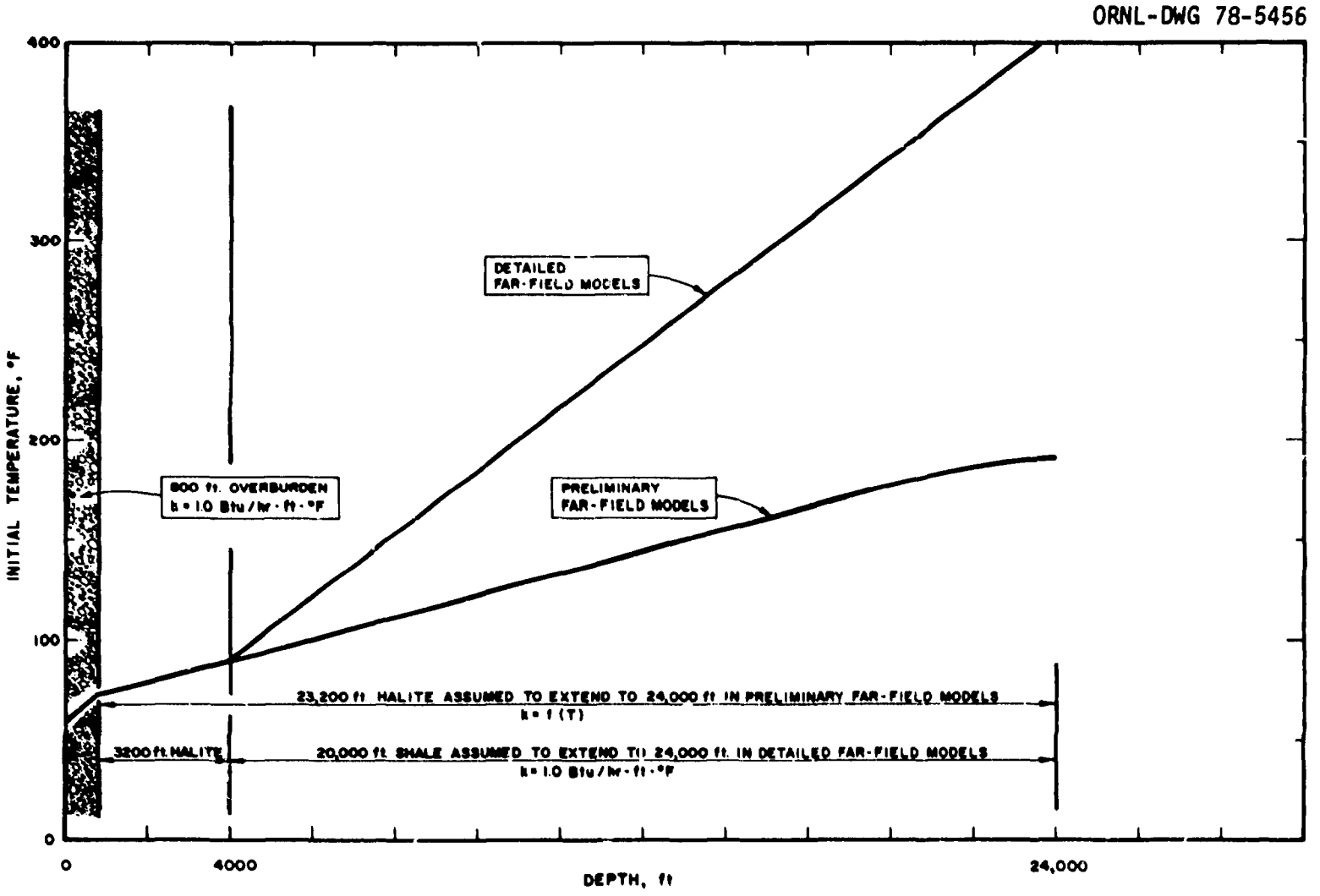

Fig. 6.2. Geothermal gradients.

for which the thermal conductivity is a function of temperature; these gradients are more apparent where larger temperature deviations occur.

A geothermal gradient of 0.016°F/ft was calculated for the overburden and shale, whereas 0.0054°F/ft was calculated for the salt region. This agrees reasonably well with the range of geothermal gradients of 0.006 to 0.06°F/ft (ref. 26) in the continental United States. Jessop et al.[27] complied and listed the geographic coordinates, depth, thermal conductivity, geothermal flux, geothermal gradient, and other pertinent stratigraphic information for each location.

7. PRELIMINARY COMPARISONS OF SF AND HLW AT 150 kW/ACRE AND 3.5 kW/CANISTER

It was desired to determine the effect of the difference in decay rates of SF and HLW by direct comparison at an initial heat load of 150 kW/acre and 3.5 kW/canister, which was previously found acceptable for HLW.[28] Two basic heat transfer models were used in the preliminary analysis of the terminal storage of radioactive waste material in salt repositories. A two-dimensional far-field model that uses a homogenized heat source was created. This model, which includes the repository region, represents an area of over 25 sq miles and is thought to be adequate for predicting temperatures in long-term transients outside the immediate vicinity of the repository. However, this model does not have the capability to indicate local maximum salt temperatures surrounding each canister. For this reason, a near-field or unit-cell model was created in which a pro rata share of the total repository area was allocated to each canister. The unit-cell model is based on a single canister heat load of 3.5 kW for both SF and HLW. The area of the far-field model, which encompasses over 16,000 acres, represents the surface area of the total repository; the area of the unit-cell model represents only the area associated with a single canister.

The comparative models for the preliminary cases were supplied with identical boundary conditions and initial heat sources, and only the decay rates of the SF and HLW heat sources were different.

The models and the geometry have been kept simple; properties and initial heat are identical for the purpose of comparing temperature increases in the repository brought about from the storage of SF or HLW. The two-dimensional models should be adequate for comparison of far-field effects and for rough estimations of maximum anticipated temperatures in the salt. The unit-cell and far-field models were used to analyze four preliminary cases: (1) far-field with SF (case A), (2) far-field with HLW (case B), (3) unit-cell with SF (case C), and (4) unit-cell with HLW (Case D), as summarized in Table 7.1.

Table 7.1. Two-dimensional R,Z computer models for preliminary comparisons — cases A through D

Item	Case A	Case B	Case C	Case D
10-year-old waste type	SF	HLW	SF	HLW
Model	Far-field	Far-field	Unit-cell	Unit-cell
Transient, years	1.0×10^5	1.0×10^5	1500	4500
Thermal load, kW/acre	150	150	150	150
Source heat at 10 years, kW	133,000	133,000	3.5	3.5
Source area, ft^2	3.85×10^7	3.85×10^7	1.40	1.40
Source height, ft	10	10	10	10
Source volume, ft^3	3.85×10^8	3.85×10^8	14.00	14.00
Initial HGR, Btu/year·ft^3	10,333	10,333	7.49×10^6	7.49×10^6
Number of canisters	38,000	38,000	1	1
Peak ΔT, °F	259	218	337	301
Time to reach peak ΔT, years	40	60	20	40

7.1 Two-Dimensional Far-Field Model Used in the Preliminary Comparisons — Cases A and B

One-dimensional preliminary parametric studies indicated that a two-dimensional model with the radial boundary extending to 15,000 ft and the depth extending to 24,000 ft is needed in order to obtain near isothermal boundaries throughout the 100,000-year transient.

The 133-MW heat source used in the far-field model for cases A and B extends radially outward to 3500 ft; it begins at 1990 ft below the surface and extends to 2000 ft. The thermal properties of the heat generation zones are assumed to be the same as those of the salt because only 1% of the entire volume actually consists of material other than salt. Repository medium temperatures are of primary interest in this investigation, and properties assumed for the waste will not affect these results.

The top surface of the overburden is assumed to be cooled with 60°F air, which is formulated in the model as a forced convection surface boundary condition with a heat transfer coefficient of 4 Btu/hr·ft^2·°F. The calculated initial temperature distribution was imposed on the model as a function of the depth below the surface. A constant geothermal flux of 0.016 Btu/hr·ft^2 was imposed and maintained at the base of the model. The outer radial boundaries were considered to be adiabatic.

7.2 Two-Dimensional Unit-Cell Model Used in Preliminary Comparisons — Cases C and D

The near-field temperatures were calculated with the use of a two-dimensional cylindrical (R,Z) heat transfer model for cases C and D that has an adiabatic boundary at a radius of 18 ft, simulating a single unit cell and an initial canister heat load of 3.5 kW. The 18-ft unit-cell radius was assumed on the basis of a thermal loading of 150 kW/acre. The depth of the model is taken to be only 4000 ft because long-term results are not pertinent in the near-field calculations. The cylindrical heat source used in this model has a 0.67-ft radius and is located vertically between 1990 and 2000 ft, which is the same vertical location as in the far-field model.

7.3 Midplane Temperature Increases Calculated for the Preliminary Comparisons

Salt temperature increases obtained in the repository are shown in Fig. 7.1 as a function of time for all four preliminary cases. These peak rises occur on the horizontal midplanes at a depth of 1995 ft at the centerline in cases A and B and at the salt-waste interface at a depth of 1996 ft in cases C and D. A maximum increase in temperature of 337°F occurring 40 years after emplacement was noted in case C for SF, which corresponds to a maximum temperature of 416°F. A maximum temperature increase of 301°F for the HLW occurs 20 years after emplacement, yielding a maximum temperature of 379°F in case D. After 40 years, the peak increase in case D is reduced to 279°F. Peak temperature increases in the SF lagged the peaks for the HLW by 20 years in both the far-field and unit-cell calculations. The far-field analysis yielded a 41°F higher peak for the SF (case A) than for the HLW (case B), and a 36°F higher peak was determined for the unit-cell calculation. A 5°F increase is still present for SF in case A even after 100,000 years, whereas less than 1°F increase was noted at the same time for HLW in case 3.

Although Fig. 7.1 shows that the temperature increases resulting from SF and HLW decrease after 40 and 20 years, respectively, the net difference between the two curves increases with time, achieving a maximum temperature difference of about 150°F after 600 years. Peaks occur earlier in the unit-cell analysis than in the far-field analysis because the adiabatic boundary on the relatively small unit-cell radius restricts radial heat flow and because the unit cell has a lower heat capacity and causes the peak to be reached sooner.

Figure 7.2 shows the increase in temperature at a depth of 2000 ft on the edge of a repository containing either SF or HLW. The edge of the repository referred to in Fig. 7.2 is at a radius of 3500 ft. A peak temperature rise of 115°F is produced 55 years after emplacement of SF, whereas a peak rise of 98°F is produced in 35 years in the repository containing HLW.

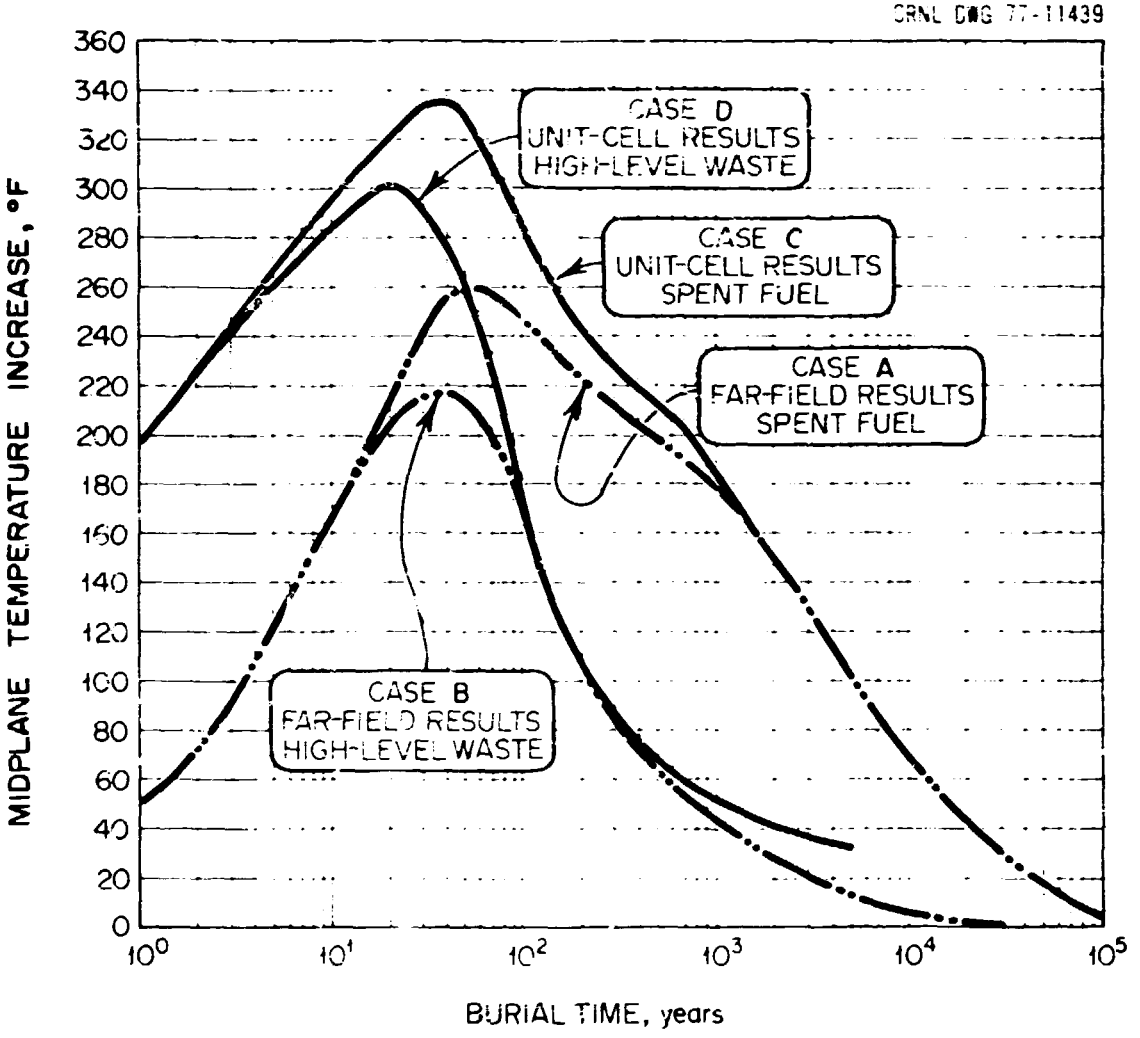

Fig. 7.1. Midplane temperature increases in salt as functions of burial time for cases A, B, C, and D.

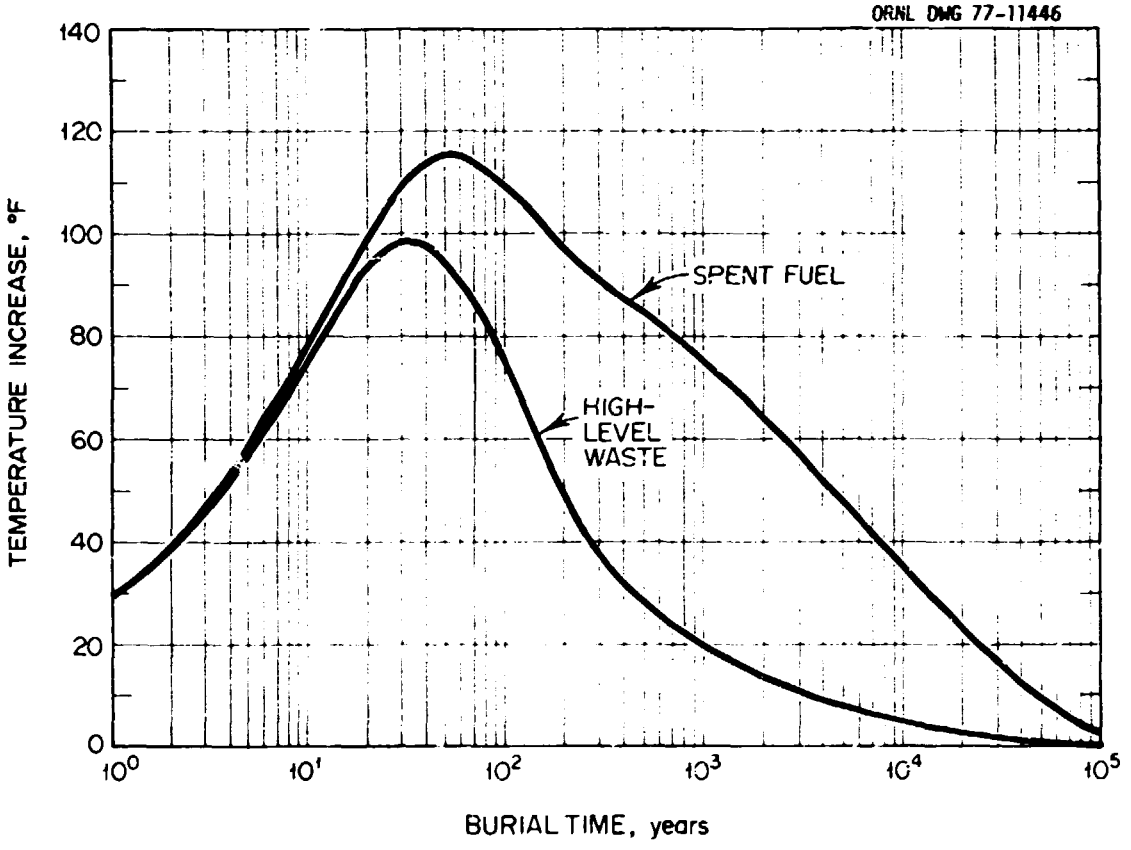

Fig. 7.2. Temperature increases at a depth of 2000 ft at the edge of a repository containing SF or HLW as a function of burial time.

8. HEAT TRANSFER MODELS FOR DETAILED COMPARISONS OF SF STORED AT 60 kW/ACRE AND 0.55 kW/CANISTER AND HLW STORED AT 150 kW/ACRE AND 2.1 kW/CANISTER

From the results of the preliminary comparisons, it was found that when SF and HLW are stored with the same initial heat load of 150 kW/acre and canister heat of 3.5 kW, the temperature rises produced are about 20% higher for SF than for HLW. It was necessary to reduce the initial heat load of the 10-year-old SF by 60% in order to produce corresponding far-field thermal effects (accumulative thermal energy and upheaval) as predicted for the 10-year-old HLW initially loaded at 150 kW/acre. The initial heat production rate and the heat source volumes for both the unit-cell and far-field models were assumed to be identical in the prelimirary models discussed in Sect. 7. The detailed models are based on heat production rates at the time of burial of 2.1 kW/canister and 150 kW/acre for the HLW and 0.55 kW/canister and 60 kW/acre for the SF as contemplated in current repository design concepts. One-dimensional far-field models were formulated to make parameter studies in transient analysis and to provide the initial temperature distribution from steady-state analysis.

Two- and three-dimensional unit-cell models were formulated to study the near-field temperature increases associated with a single canister. One- and two-dimensional far-field models were created and used primarily to predict the temperature increases remote from the heat source such as the earth's surface or several thousand feet from the repository. A multiple row model was developed as a second supportive two-dimensional far-field model and provides some correspondence between the unit-cell and far-field models.

The three-dimensional models using Cartesian geometry were originally created for the single purpose of providing the capability of modeling a repository room with internal heat transfer between the floor and ceiling.

Sections 8.1 through 8.4 are devoted to the comparisons of temperature increases incurred from storage of either SF or HLW at the previously specified heat rates. The pertinent characteristics of the nine cases run in the detailed analysis are summarized in Table 8.1. Intimate contact has been assumed between the heat source and the solid salt in all of the unit-cell models used in this study. A conservative steady-state calculation

Table 8.1. Computer models for detailed comparisons — cases 0 through 7

Item	Case 0	Case 00	Case 1	Case 2	Case 3	Case 4	Case 5	Case 6	Case 7
10-year-old waste type	SF	HLW	SF	HLW	SF	HLW	SF	HLW	HLW
Configuration			2D	2D	2D	2D	3D	3D	2D multiple row
Model	Far-field	Far-field	Far-field	Far-field	Unit-cell	Unit-cell	Unit-cell	Unit-cell	Far-field
Coordinate system			*RZ*	*RZ*	*RZ*	*RZ*	*XYZ*	*XYZ*	*XZ*
Transient, years	1.0×10^5	1.0×10^5	1.0×10^5	1.0×10^5	100	200	35	35	100
Thermal load, kW/acre			60	150	60	150	60	150	150
Source heat at 10 years, kW			133,000	133,000	0.55	2.10	0.55	2.10	133,000
Source area, ft^2	1	1	9.66×10^7	3.85×10^7	2.18	2.18	2.18	2.18	7.82/canister
Source height, ft	12	8	12	8	12	8	12	8	8
Source volume, ft^3			1.16×10^9	3.08×10^8	26.18	17.45	26.18	17.45	62.56/canister
Source HGR at 10 years, $Btu/yr \cdot ft^3$	3432	12,916	3432	12,916	6.27×10^5	3.60×10^6	6.27×10^5	3.60×10^6	1.0×10^6
Source radius, ft			5544	3500	0.83	0.83			
Model radius, ft			24,000	15,000	11.26	13.92			
Model height, ft			0-24,000	0-24,000	0-4000	0-4000	1000-3000	1000-3000	800-4000
Model width, ft							39	39	4000
Model depth							2.56	3.91	Infinite
Canisters			242,259	63,333	1	1	1	1	63,333
Peak ΔT, °F	100	224	101	223	105	269	113	301	239
Time to reach peak, years	60	35	60	35	50	25	35	20	27

shows that no more than 20°F radial ΔT may occur across a 2-in. annular ring of solid halite. Crushed salt has only 10% of the initial thermal conductivity of solid salt. Using a 2-in. backfill of crushed salt in the annular volume could increase surface temperatures of the canister by 200°F. The temperature of the undisturbed salt, however, would remain unchanged. Experiments[29] indicate that the salt will eventually resolidify; the rate of resolidification is dependent on temperature, moisture content, and pressure. This theory may be confirmed by the in situ rock mechanics experiments using electrical heat sources in a domed salt formation which are currently being planned by the Office of Waste Isolation.

8.1 One-Dimensional Far-Field Models (Cases 0 and 00) and Results

Simple one-dimensional far-field models were formulated assuming an 800-ft overburden with constant thermal properties, a 3200-ft halite strata that extends 4000 ft below the earth's surface, and with shale extending to the base of the model at a depth of 24,000 ft. The properties of this stratigraphy are listed in Sect. 6. The boundary conditions used on this model are a forced-convection surface heat transfer coefficient of 4 Btu/hr·ft^2·°F to 60°F ambient air and a geothermal flux of 140 Btu/yr·ft^2 imposed at the 24,000-ft depth. These same boundary conditions and stratigraphy have been employed on the two-dimensional far-field models. The primary purpose of the one-dimensional models was to obtain a steady-state temperature distribution utilizing only the geothermal flux; this model requires no additional heat source. This temperature distribution, as previously shown in Sect. 4, has been used as the initial temperature distribution in all models used in the detailed analysis.

The one-dimensional models have also been used in parametric studies to establish the extent of the boundaries necessary for the far-field models based on the rate of temperature propagation. The initial volumetric heat generation rate used in these cases is the same as that used for the two-dimensional far-field sources developed in Sect. 4. The initial volumetric heat generation rate for a homogenized fuel zone containing 10-year-old SF is 3432 Btu/yr·ft^3; this zone extends from a depth of 2010 ft to 2022 ft, which simulates the active canister height of 12 ft.

The initial volumetric heat generation rate for HLW is 12,869 Btu/yr·ft^3; this zone extends from a depth of 2010 ft to 2018 ft, which simulates an 8-ft active fuel height.

Initial temperature distributions — the main purpose for running these models — were obtained from steady-state analysis of the preliminary and detailed models. The results have been discussed in Sect. 6.3 and shown in Fig. 6.2. In addition, parametric runs have been made with these models to establish model boundary limits. Peak temperature increases obtained as a result of these runs at various depths below the surface for both SF and HLW are shown in Fig. 8.1. These temperature increases do not represent maximum increases (ΔTs) because of the assumption of homogenization of the heat generating zone, but they show the general temperature distribution expected remote from the heat source. These models show that there is only a small temperature increase 500 ft away from the source at their peaking times.

8.2 Two-Dimensional Homogenized Far-Field Model (Cases 1 and 2) and Numerical Results

The two-dimensional far-field models are designed to obtain temperature increases at remote points from the repository for the purpose of environmental or ecological justification. The models must extend from the repository to the earth's surface. From one-dimensional parametric studies, it was found that the lower axial boundary must be about six times the depth of the repository. The radial boundary of the model must extend to about four repository radii in order to maintain isothermal boundaries during a 100,000-year transient with adiabatic boundary conditions.

The first 800-ft depth of the models is assumed to be overburden with constant physical properties. Pure halite is assumed to exist from 800 ft to a depth of 4000 ft. The thermal conductivity of the halite is assumed to be a function of temperature. Shale is assumed to begin at an elevation of 4000 ft and extend to 24,000 ft. Physical properties used in these models are given in Sect. 6.1.

A geothermal heat flux of 140 Btu/yr·ft^3 is imposed at the base of the model, and heat is constantly removed at the earth's surface by forced convection with a heat transfer coefficient of 4.0 Btu/hr·ft^2·°F to 60°F ambient air.

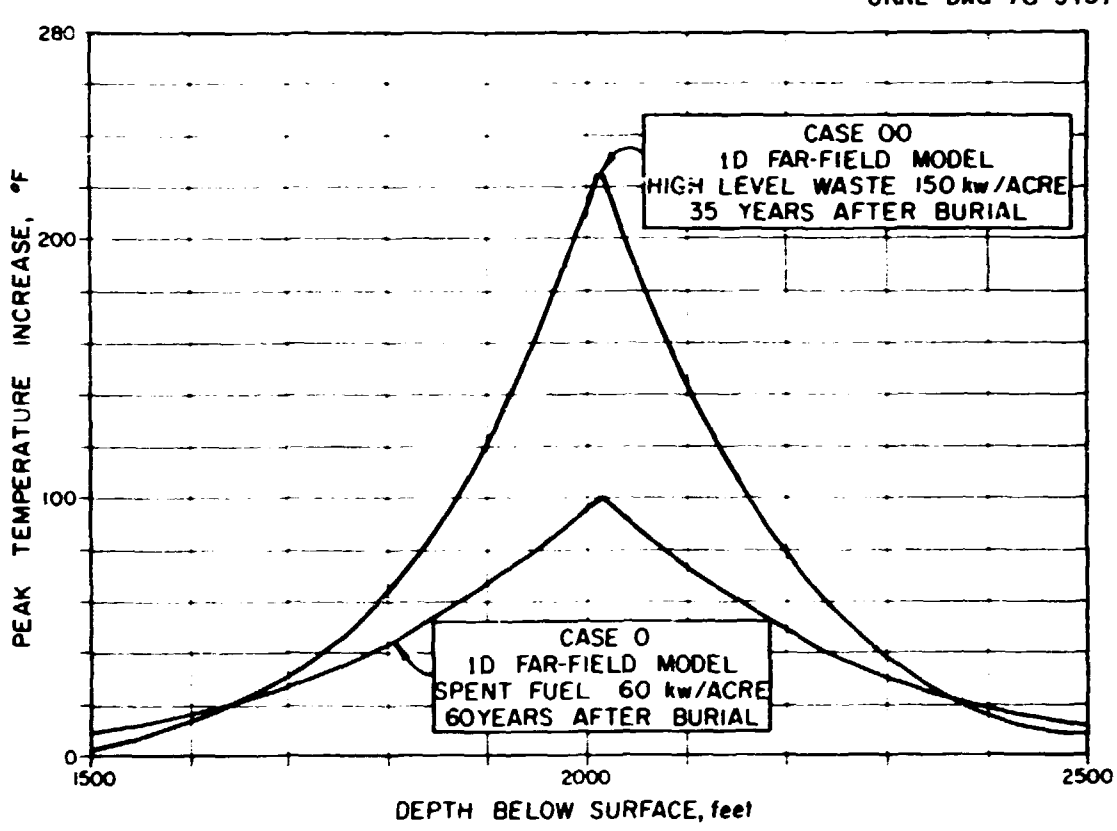

Fig. 8.1. Peak temperature increases in one-dimensional salt models as functions of depth for SF stored at 60 kW/acre and HLW stored at 150 kW/acre.

The two-dimensional far-field model containing SF for case 1 is shown in Fig. 8.2. The 133-MW source in this model is a right circular cylinder that is 12 ft in height, has a radius of 5544 ft, and has an initial volumetric heat generation of 3432 Btu/yr·ft^3. The heat source extends from a depth of 2010 ft to a depth of 2022 ft. The repository area containing the SF is about 2217 acres, based on a total heat load of 133 MW stored at 60 kW/acre. This model has an adiabatic boundary at a radius of 24,000 ft.

A similar far-field model loaded with HLW at 150 kW/acre is used for case 2 as shown in Fig. 8.3. This model has the same boundary conditions as described for case 1 except that the adiabatic radial boundary is imposed at a radius of 15,000 ft. The repository area in this case is 883 acres, based on a total heat load of 133 MW stored at 150 kW/acre.

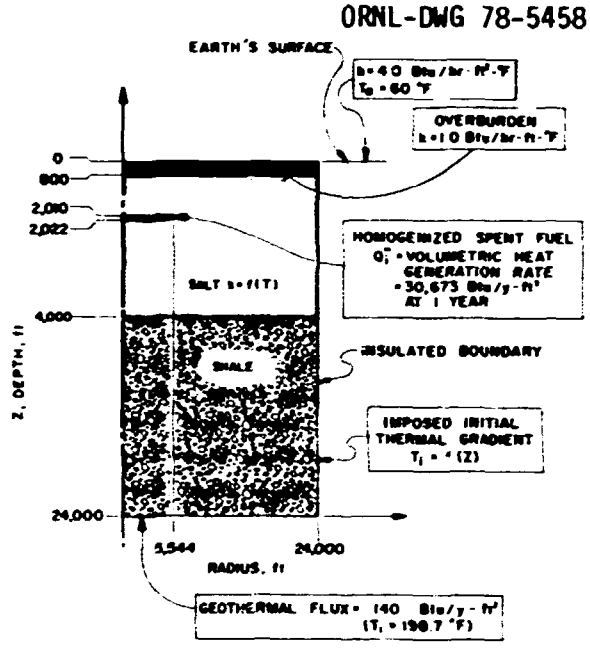

Fig. 8.2. Two-dimensional homogenized far-field heat transfer model of a 2217-acre SF repository.

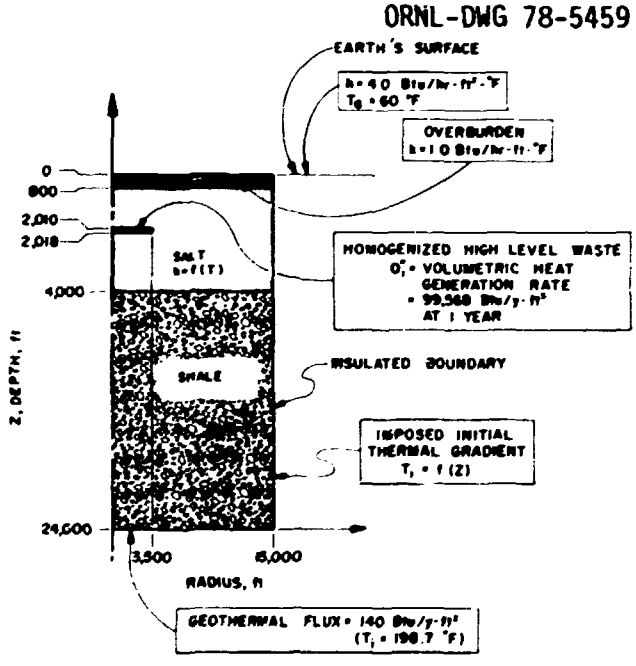

Fig. 8.3. Two-dimensional homogenized far-field heat transfer model of an 883-acre HLW repository.

The source in this model is bounded at a radius of 3500 ft and extends from a depth of 2010 ft to a depth of 2018 ft. The initial volumetric heat generation of the source is 12,916 Btu/yr·ft^3.

Temperature increases (ΔTs) as functions of depth below the earth's surface for times up to 30,000 years have been determined for the storage of SF loaded at 60 kW/acre (case 1) as shown in Fig. 8.4. Similar distributions have been obtained for HLW loaded at 150 kW/acre (case 2) as shown in Fig. 8.5. On comparison, it is apparent that initially the HLW produces much higher temperature increases, but after about 300 years, the ΔTs in the HLW repository are much lower than in the SF repository. Note also that the resulting temperature distribution is not quite symmetric. Points above the source are cooler than below it in both the SF and HLW cases because of the cooling effect of the atmosphere. A peak temperature of 100°F was obtained for SF 60 years after burial, whereas a peak temperature increase of 223°F was obtained for HLW 35 years after burial. The temperature distributions in Z direction are practically identical with those obtained from the one-dimensional analysis. Because the one-dimensional cases are much simpler and cheaper to run, they can be used instead of two-dimensional models whenever temperature distribution as a function of depth is the only interest.

Figure 8.6 shows the temperature increases at the edge of the repository containing SF loaded at 60 kW/acre as a function of the radial distance from the centerline for various times up to 30,000 years. Figure 8.7 shows the same relationships at the edge of a repository containing HLW loaded at 150 kW/acre. It is quite apparent from comparison of these two figures that the temperature increase incurred by the SF exceeds that incurred by the HLW after 500 years. In both cases, the ΔT at the repository midplane remains quite flat over most of the repository area, which indicates little radial heat transfer near the center of the repository. At a radial distance of about 600 ft from the repository containing SF, a midplane ΔT of no more than 15°F is noted at any point in time. A similar observation is made for the case of the HLW. Here the ΔT is less than 10°F within 500 ft of the repository edge. This observation is very important because it reinforces the assumption of adiabatic radial boundary conditions on the unit-cell models.

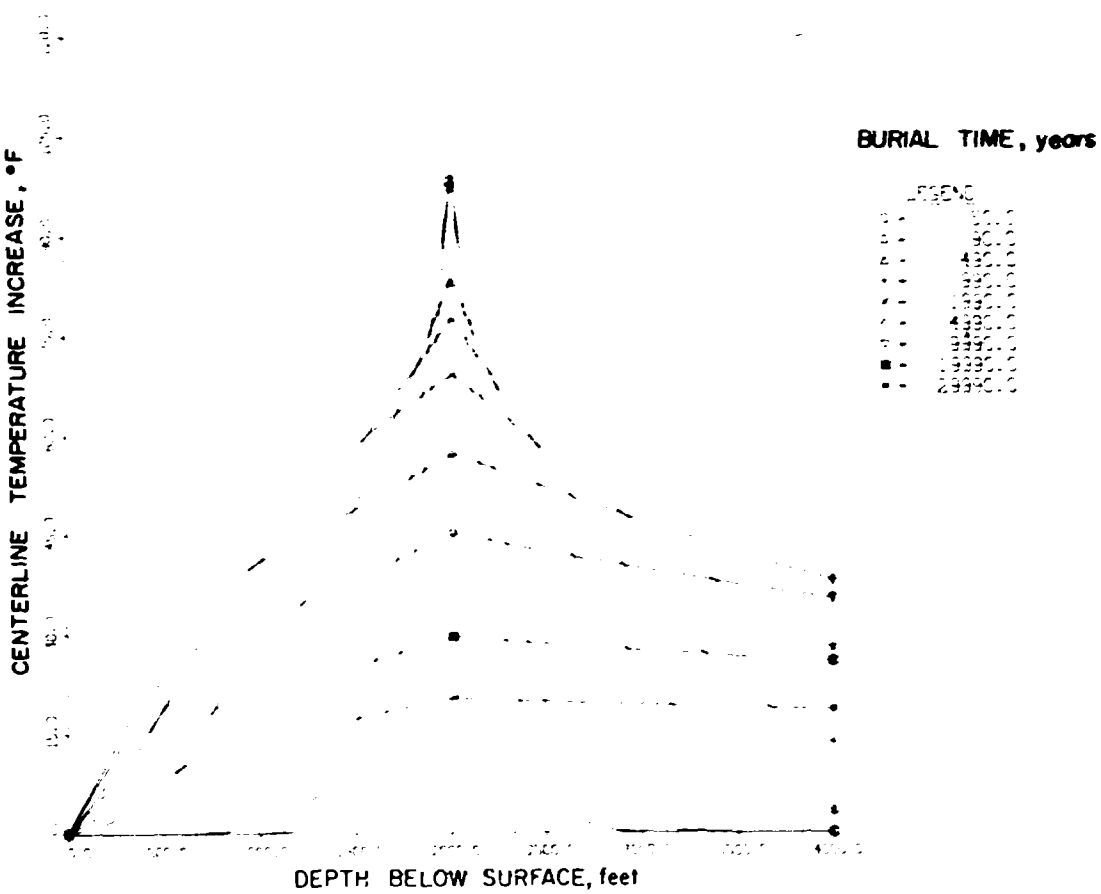

Fig. 8.4. Centerline temperature increase in a two-dimensional far-field model at various imes as functions of depth resulting from the storage of SF at 60 kW/acre.

Figure 8.8 shows the ΔT at various depths along the centerline of a repository loaded with SF at 60 kW/acre as functions of time. Figure 8.9 shows the same profiles for HLW loaded at 150 kW/acre. The same information is shown in these plots as was presented in Figs. 8.4 and 8.5, but the emphasis is on behavior of temperature with respect to time.

At a depth below about 1500 ft, the ΔTs in the HLW repository are greater than or equal to the ΔT obtained from the SF repository, but at depths less than 1500 ft the ΔTs in the HLW repository are less than those found in the repository containing the SF. At peaking time (35 years after burial) the ΔT in the HLW is about 2.3 times that found in the SF, but at about 300 years after burial they are about the same (85°F), and at longer times the ΔTs are greater in the SF repository than in the HLW repository.

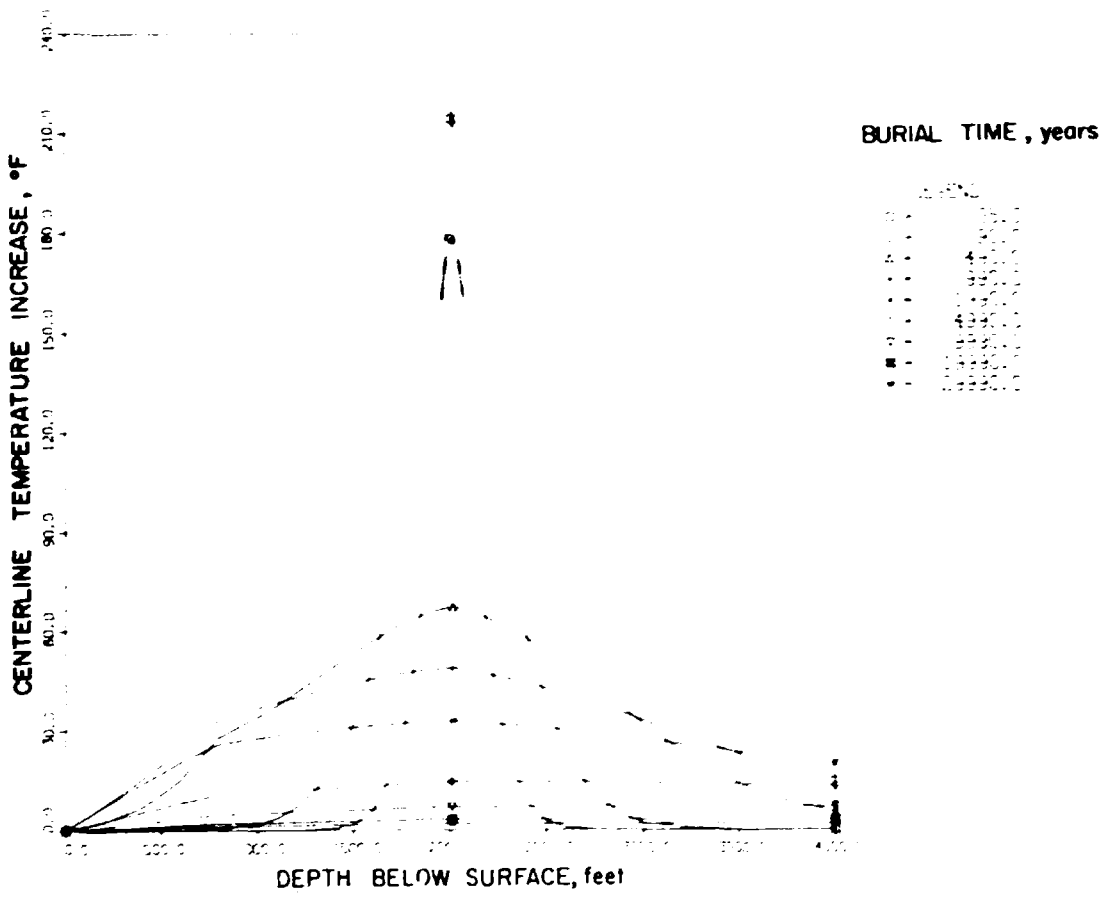

Fig. 8.5. Centerline temperature increase in salt in two-dimensional far-field model at various times as function of depth resulting from the storage of HLW at 150 kW/acre.

Figure 8.10 shows the midplane temperature increases incurred from the storage of SF at 60 kW/acre as functions of time at various radial locations. Similar profiles have been obtained for HLW stored at 150 kW/acre and are shown in Fig. 8.11. These plots present the same information as Figs. 8.6 and 8.7, in which the main interest was on the temperature distribution at the edge of the repository. Here, the emphasis is on the variation of the temperature increase with time at a particular location. The main differences observed between the SF and the HLW is that the HLW peaks more quickly with a higher temperature increase and returns more quickly to the initial conditions. The ΔT in the SF repository peaks more slowly and holds close to the peak for a longer period than the HLW. Both curves have a noticeable drop in the temperature increase at the edge of the repository.

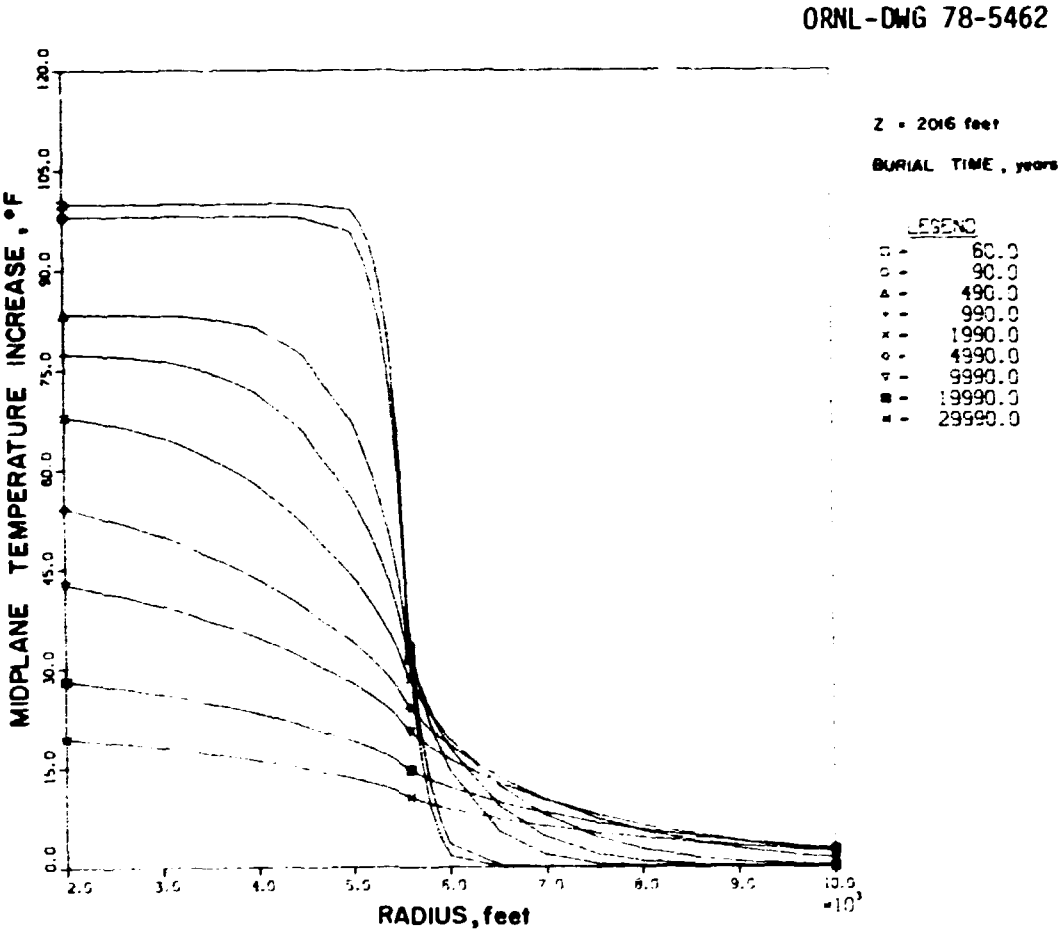

Fig. 8.6. Midplane temperature increases in salt at various times as functions of radial distance from the centerline in a repository loaded with SF at 60 kW/acre.

8.3 Two-Dimensional Unit-Cell Models (Cases 3 and 4) and Numerical Results

The two-dimensional unit-cell models were created to obtain the maximum near-field temperatures. These models extend from the surface of the earth to a depth of 4000 ft. The 4000-ft depth was chosen because in a 200-year transient, heat is not propagated in sufficient quantity to cause appreciable temperature changes at the boundaries.

Figure 8.12 shows the two-dimensional unit-cell model for a PWR spent fuel assembly as used for case 3. The heat source used in this model is emplaced as was illustrated in Fig. 4.1 with a volumetric heat generation of 6.27×10^5 Btu/yr·ft^3, 10 years after removal from the reactor as discussed in Sect. 4.3.

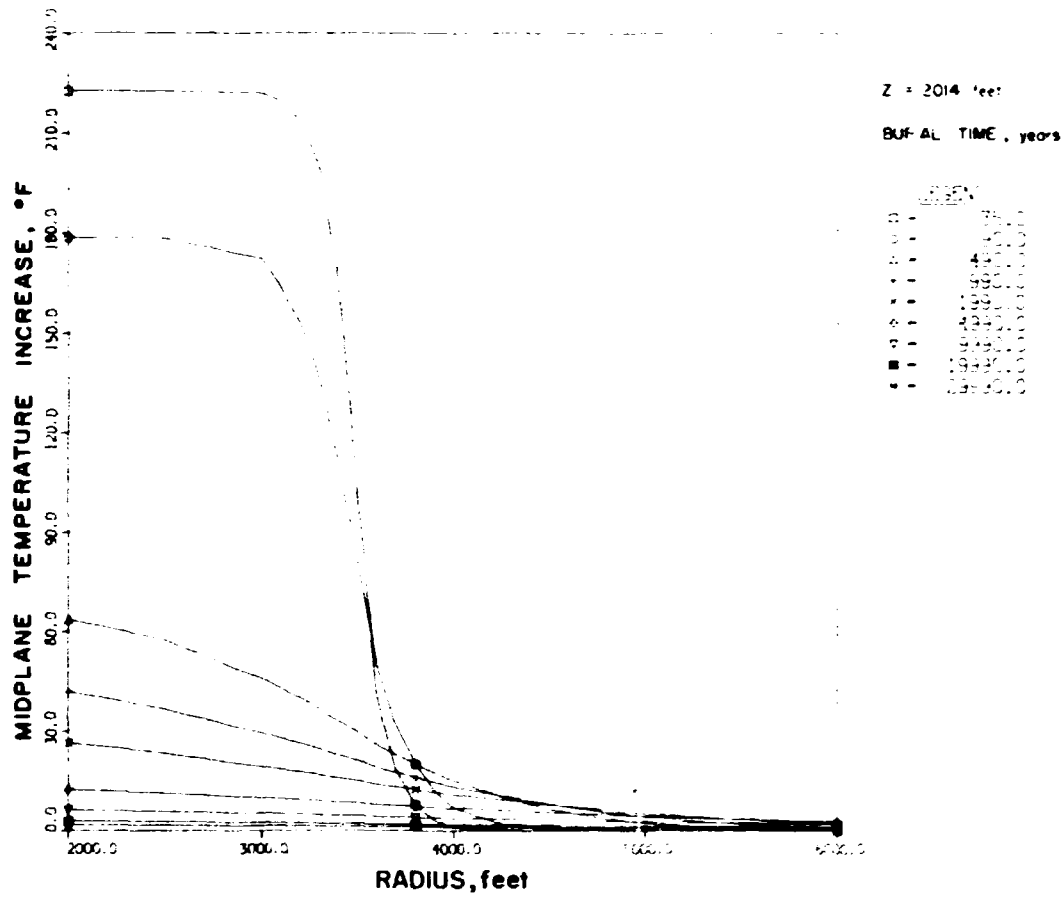

Fig. 8.7. Midplane temperature increases in salt at various times as functions of radial distances from the centerline in a repository loaded with HLW at 150 kW/acre.

The pro rata area of the 60-kW/acre SF repository associated with one fuel assembly generating 0.55 kW is 0.0092 acres (399 ft^2), which results in a unit-cell radius of 11.26 ft. The source has a radius of 0.83 ft and is located between a depth of 2010 and 2022 ft as previously described.

A similar model for use with case 4 was formulated for HLW and is shown in Fig. 8.13. The heat source used in the model has a 0.83-ft radius and extends from a depth of 2010 ft to a depth of 2018 ft; it has a volumetric heat generation of 3.60×10^6 Btu/yr·ft^3 10 years after reprocessing.

The pro rata area of the 150-kW/acre HLW repository associated with one canister generating 2.1 kW is 0.014 acres (610 ft^2), which results in a unit-cell radius of 13.92 ft.

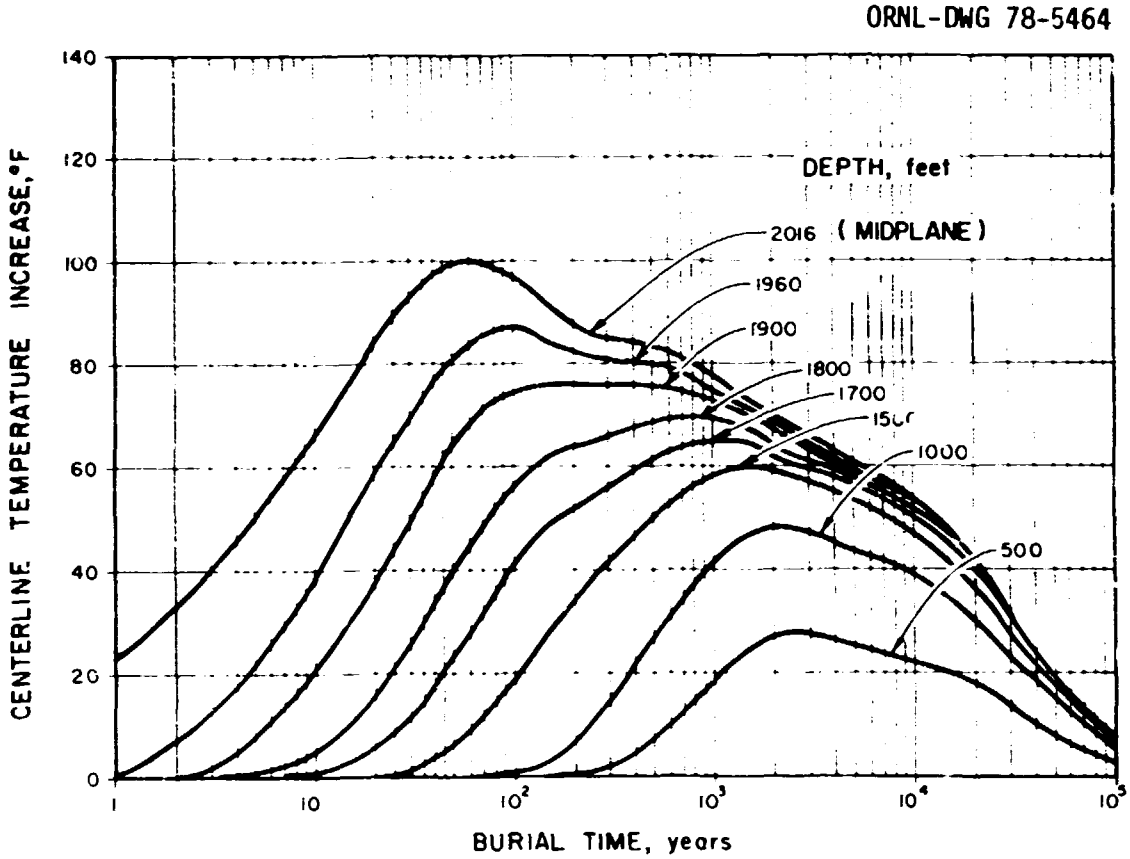

Fig. 8.8. Centerline temperature increase in salt in a two-dimensional far-field model at various depths as functions of time resulting from the storage of SF at 60 kW/acre.

The pertinent information to be obtained from these models is the maximum temperature increase (ΔT), its location, and its peaking time. As shown in Fig. 8.14, a peak maximum ΔT of 105°F was calculated for the salt about 50 years after burial in the case of SF. This maximum temperature occurs on the canister surface at a depth of 2016 ft. A similar peak maximum ΔT of 269°F was calculated for HLW at a depth of 2014 ft about 25 years after burial.

8.4 Three-Dimensional Models (Cases 5 and 6) and Numerical Results

The three-dimensional unit-cell model with no air exchange in an open room appears to be the most conservative of any of the models attempted. The three-dimensional model is designed to simulate a cell of an open room

ORNL-DWG 78-5431

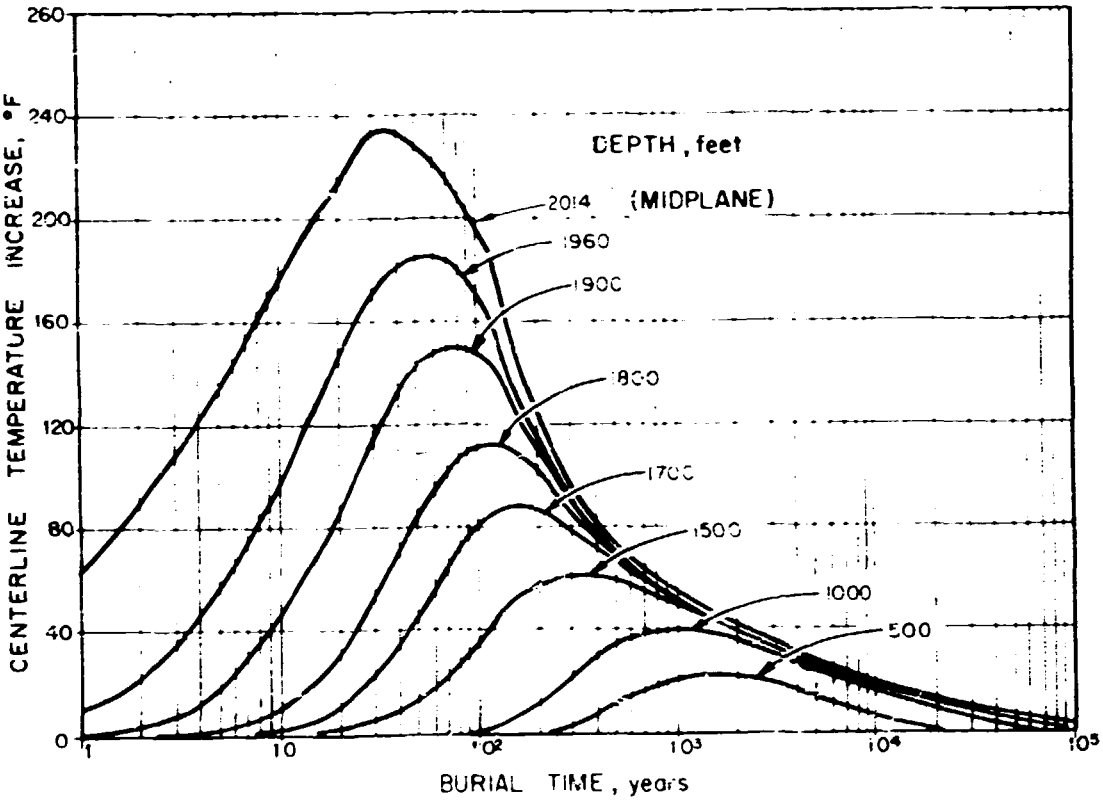

Fig. 8.9. Centerline temperature increases in salt in a two-dimensional far-field model at various depths as functions of time resulting from the storage of HLW at 150 kW/acre.

in a repository. The boundary conditions imposed on the surfaces of the room are quite important in predicting the temperatures in the salt, and several factors must be considered.

If forced air circulation is assumed, the maximum surface temperature could eventually be reduced close to the temperature of the bulk air, but flow requirements would be excessively large to accomplish this purpose. If each cell is assumed isolated, or sealed, the air eventually will assume the mean temperature of the room with only minor heat transfer due to natural convection. Therefore, a sealed room was modeled and the convection losses were conservatively neglected; only heat transfer by radiation from the warmer floor to the cooler ceiling was considered. The emissivities of both surfaces were assumed to be 0.8 (dimensionless). The retrievable mode of operation is where the room is not backfilled, although it can be sealed, with the waste material being accessible. The SF is buried so that

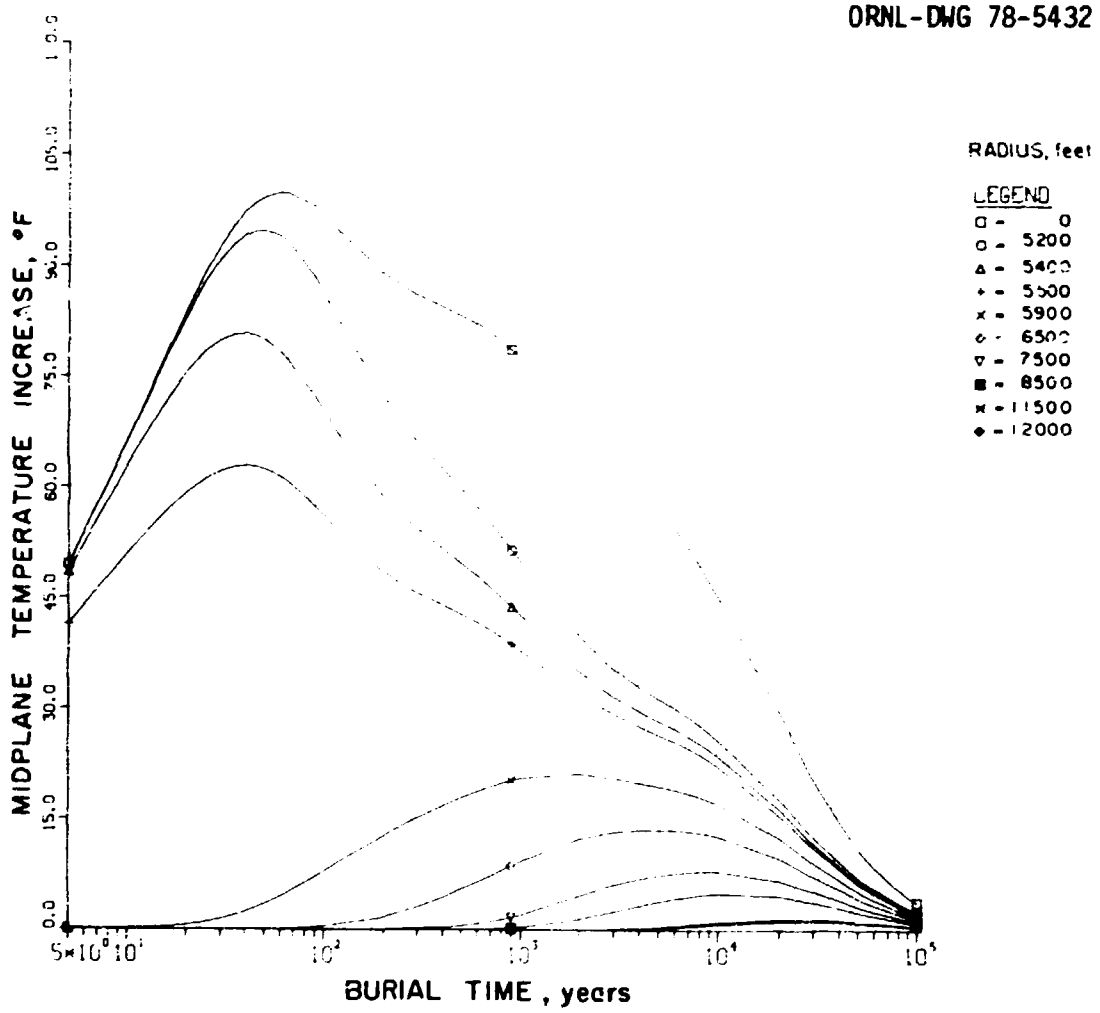

Fig. 8.10. Midplane temperature increases at various radial locations as functions of time in a repository loaded with SF stored at 150 kW/acre.

it can be retrieved for up to 25 years, whereas the period of retrievability for the HLW is 5 years. Due to these considerations, the transients for both three-dimensional models were extended to 35 years.

The three-dimensional model is shown in Fig. 8.15. In order to conserve nodes, the vertical boundaries were confined to within 600 ft of the source. Based on results achieved in the one-dimensional models, a boundary temperature of 75.8°F was placed on the upper boundary at a depth of 1400 ft, and a constant temperature of 81.8°F was imposed at the lowest boundary along with the geothermal flux at a depth of 2600 ft. This three-dimensional model is based on a rectangular layout of 60-ft pillars and

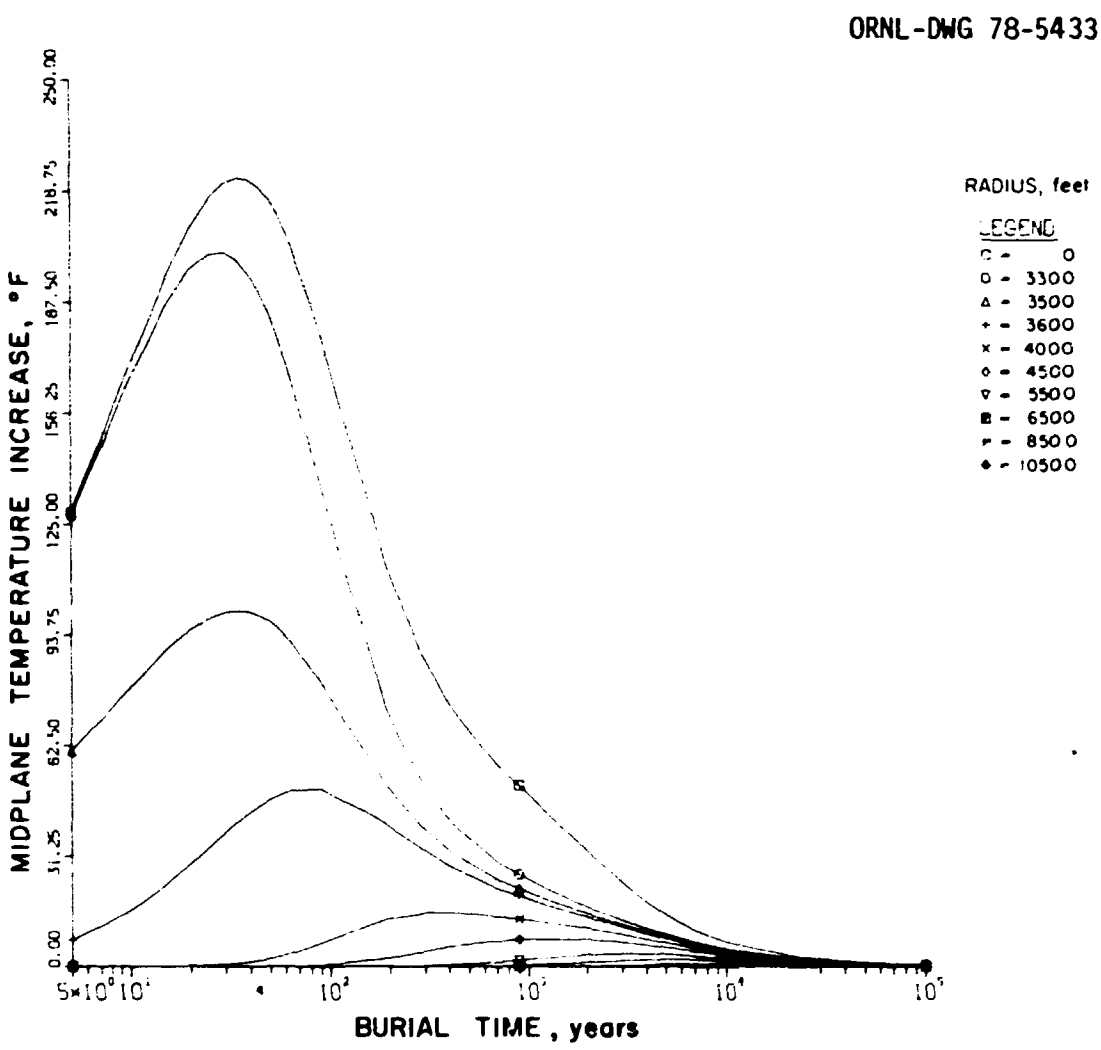

Fig. 8.11. Midplane temperature increases at various radial locations as functions of time in a repository loaded with HLW stored at 60 kW/acre.

rooms that are 18 ft wide and 18 ft high. The rooms and the canister centerlines are spaced 78 ft on center. Based on the areal heat production of 60 and 150 kW/acre, the calculated pitch between the canisters along each room for the SF is 5.12 ft and 7.82 ft for the HLW respectively. Half pitches are used in the three-dimensional models to make use of symmetry lines. The heat generation rates are the same as calculated for cases 3 and 4. The only difference is the configuration of the heat sources, which are square rather than round. Note that the salt areas in the two-dimensional unit-cell models associated with a single canister are identical to the areas in the three-dimensional models.

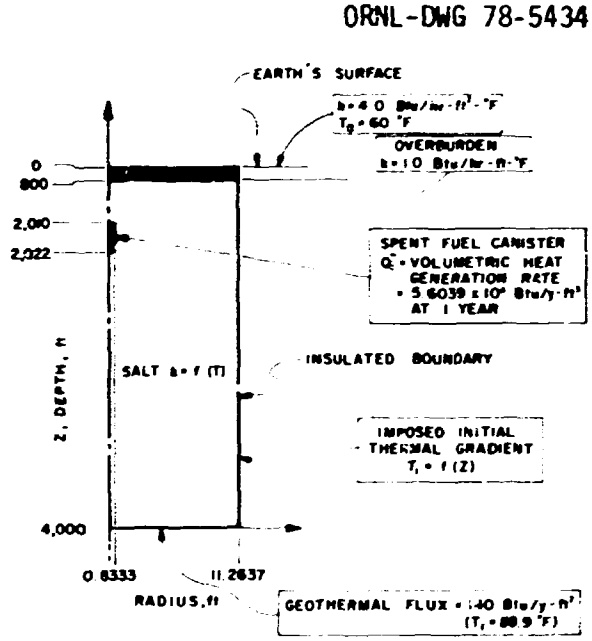

Fig. 8.12. Two-dimensional unit-cell model for storage of a canister containing a spent fuel assembly.

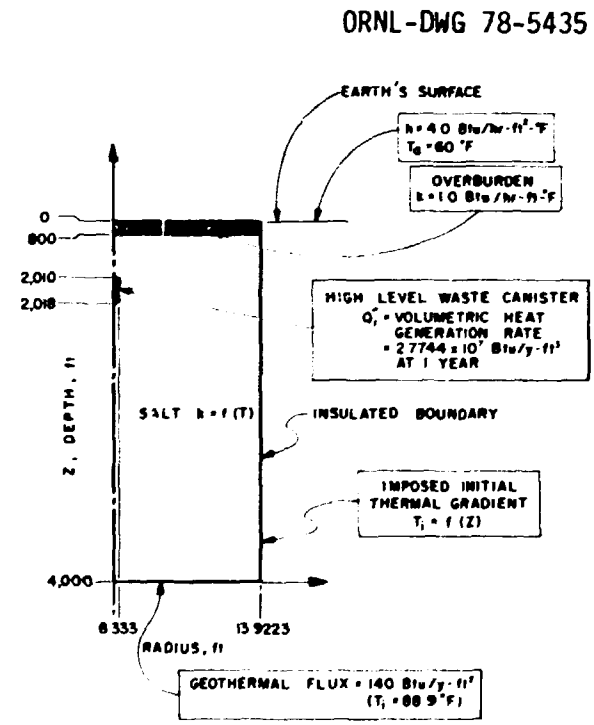

Fig. 8.13. Two-dimensional unit-cell model for storage of a canister of HLW.

ORNL-DWG 78-5436

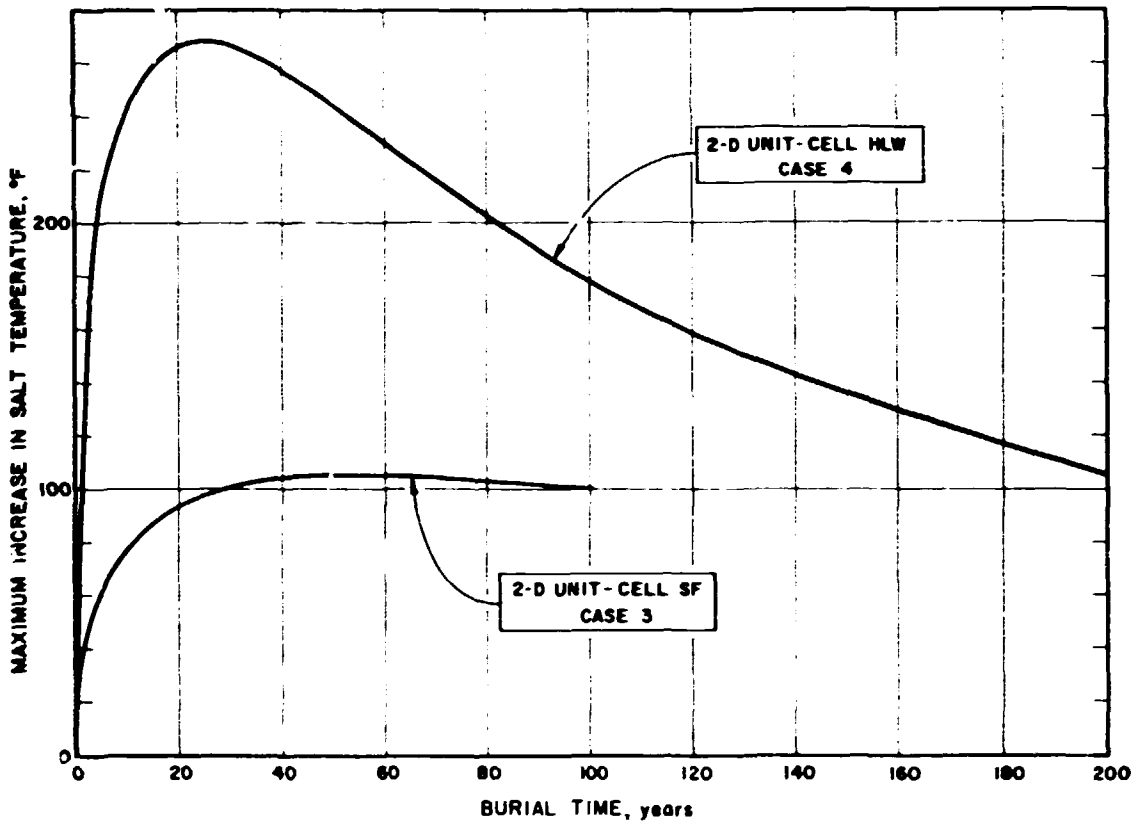

Fig. 8.14. Comparison of maximum temperature increases as functions of time in the two-dimensional unit-cell models for SF stored at 60 kW/acre and HLW stored at 150 kW/acre.

A 35-year transient was run on the three-dimensional models for cases 5 and 6. The maximum increase in the salt temperature (ΔT) for both of these cases is plotted in Fig. 8.16. The peak maximum ΔT of 113°F is obtained in case 5 for SF and occurs 35 years after burial. In case 6, the peak maximum ΔT of 301°F is obtained for HLW 20 years after burial. These peak maximum ΔTs occur on the surface of the canister at the repository midplane.

The maximum ΔT encountered for the SF in the salt after 25 years (the proposed backfilling time of the room for SF) is about 110°F, which is equivalent to a maximum temperature of 189°F. The maximum ΔT encountered for the HLW in the salt after 5 years (the proposed backfilling time for HLW) is about 260°F, which is equivalent to a maximum temperature of 339°F.

Another point of interest in the three-dimensional analysis is the maximum accessible room temperature, which occurs on the floor directly

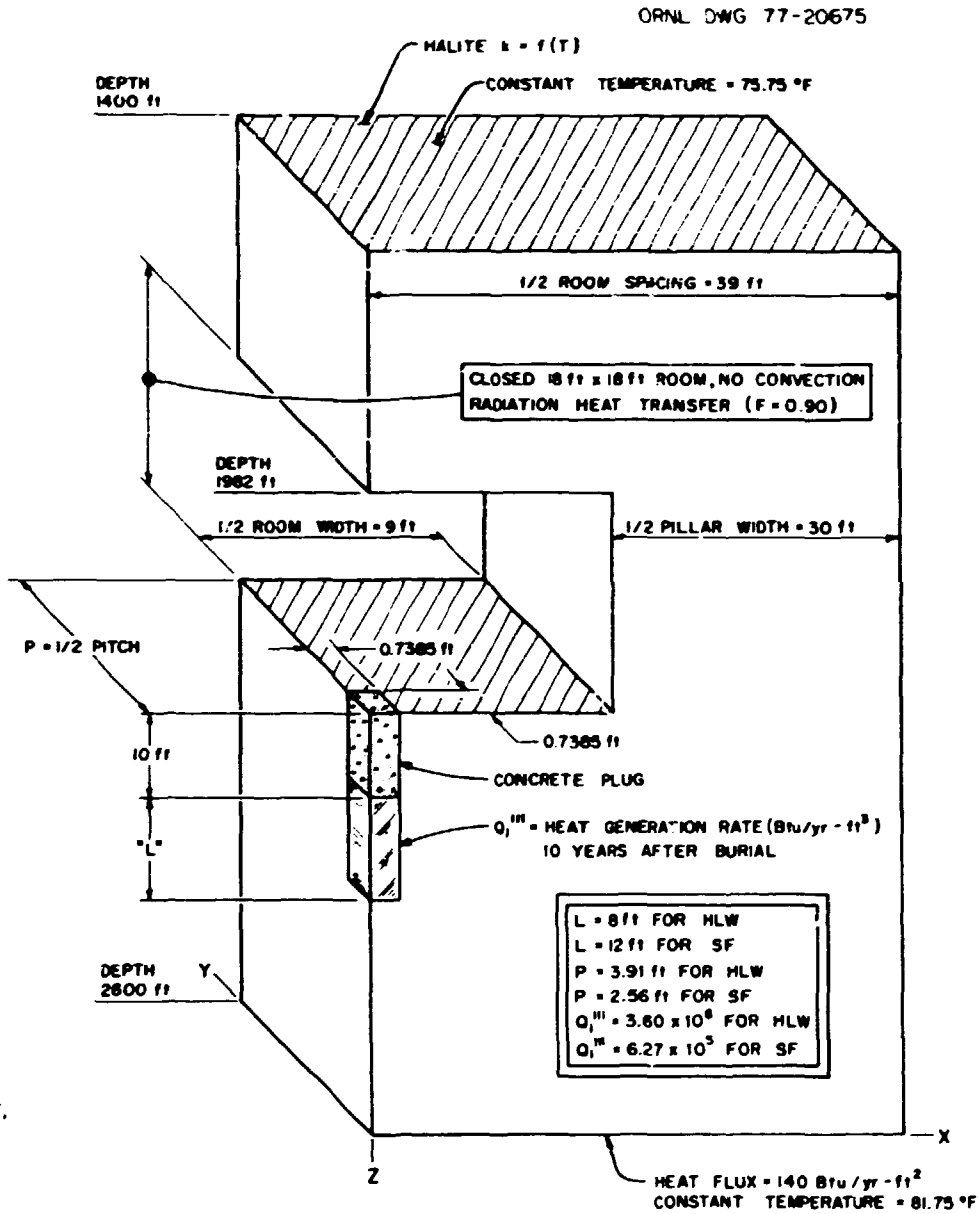

Fig. 8.15. Three-dimensional unit-cell model for a PWR spent fuel assembly or high-level waste canister.

over the waste canisters. Figure 8.17 shows the maximum floor temperature as a function of time for SF in case 5 and for HLW in case 6.

The maximum temperature obtained on the floor of the room containing HLW at the time of backfilling (5 years) is about 191°F. A peak maximum floor temperature of 294°F occurs for HLW after 35 years, or 30 years after the planned backfilling time. Rooms used to store HLW are not expected to remain open for more than 5 years.

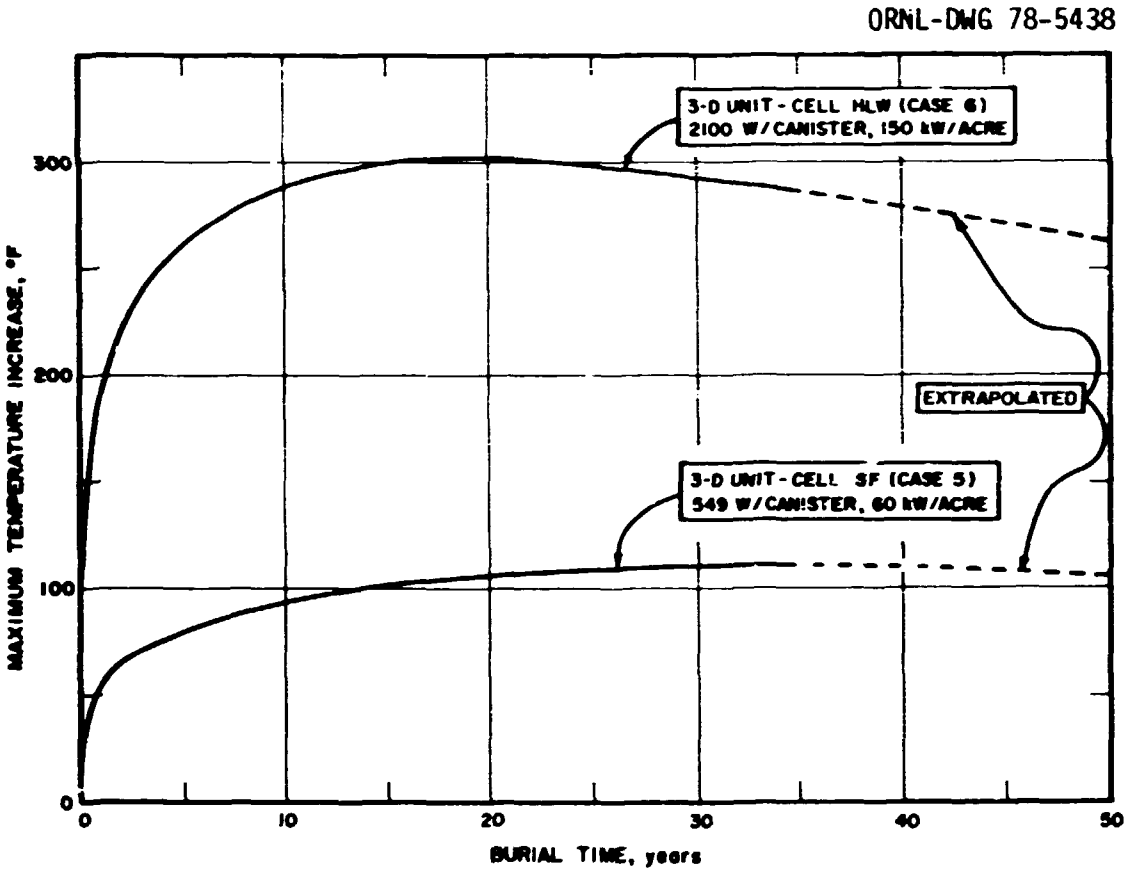

Fig. 8.16. Comparison of maximum temperature increases in salt as functions of time in the three-dimensional unit-cell models for SF stored at 60 kW/acre and HLW stored at 150 kW/acre.

A similar maximum temperature on the floor of the room containing SF at the time of backfilling (25 years) is about 161°F. A peak maximum temperature found for the floor of the room in case 5 is about 169°F, which occurs 10 years after the planned backfilling time.

In order to simulate backfilling, it would be necessary to input the temperature distribution obtained in the open room at the time of backfilling and instantaneously fill the room with crushed salt at a given temperature. All thermal properties would have to be programmed as functions of time and the thermal conductivity expressed as functions of both time and temperature to allow for the process of reconsolidation of the crushed salt. No backfilling has been assumed in the present three-dimensional models.

Contours of constant ΔTs (called isotherms here for simplicity) were generated utilizing the HEATPLOT[30] computor code for cases 5 and 6 at

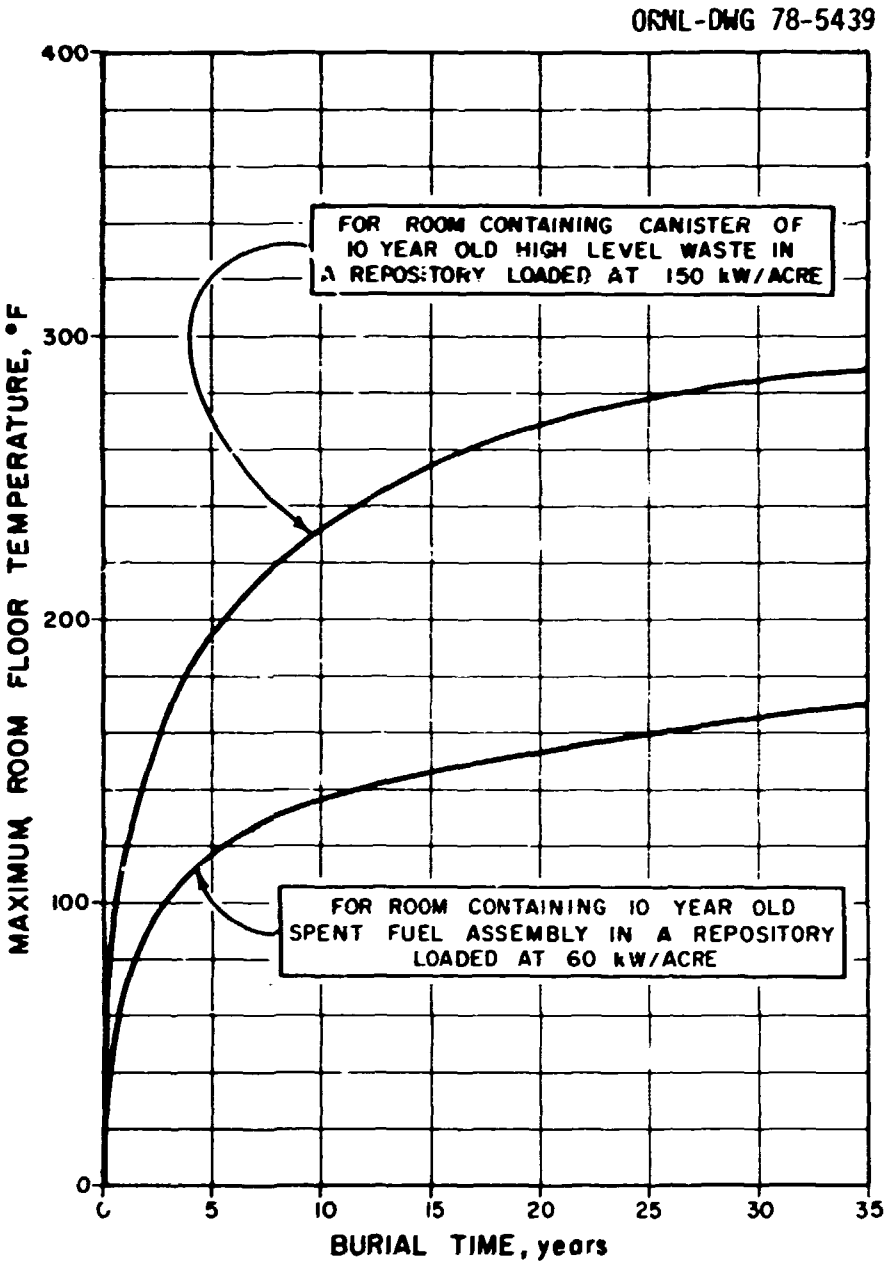

Fig. 8.17. Comparison of maximum temperature on the floor of the storage room as functions of time due to SF stored at 60 kW/acre and HLW stored at 150 kW/acre.

pertinent times in planes orthogonal to the coordinate axis passing through the center of the heat source. Figure 8.18 shows the isotherms in the *XZ* plane from case 5 for SF just prior to the scheduled backfilling, 25 years after burial. Appreciable gradients in the isotherms were observed in this plane close to the source. Figure 8.19 shows the temperature increases that occur at the horizontal midplane between canisters in a nonbackfilled

ORNL-DWG 78-5440

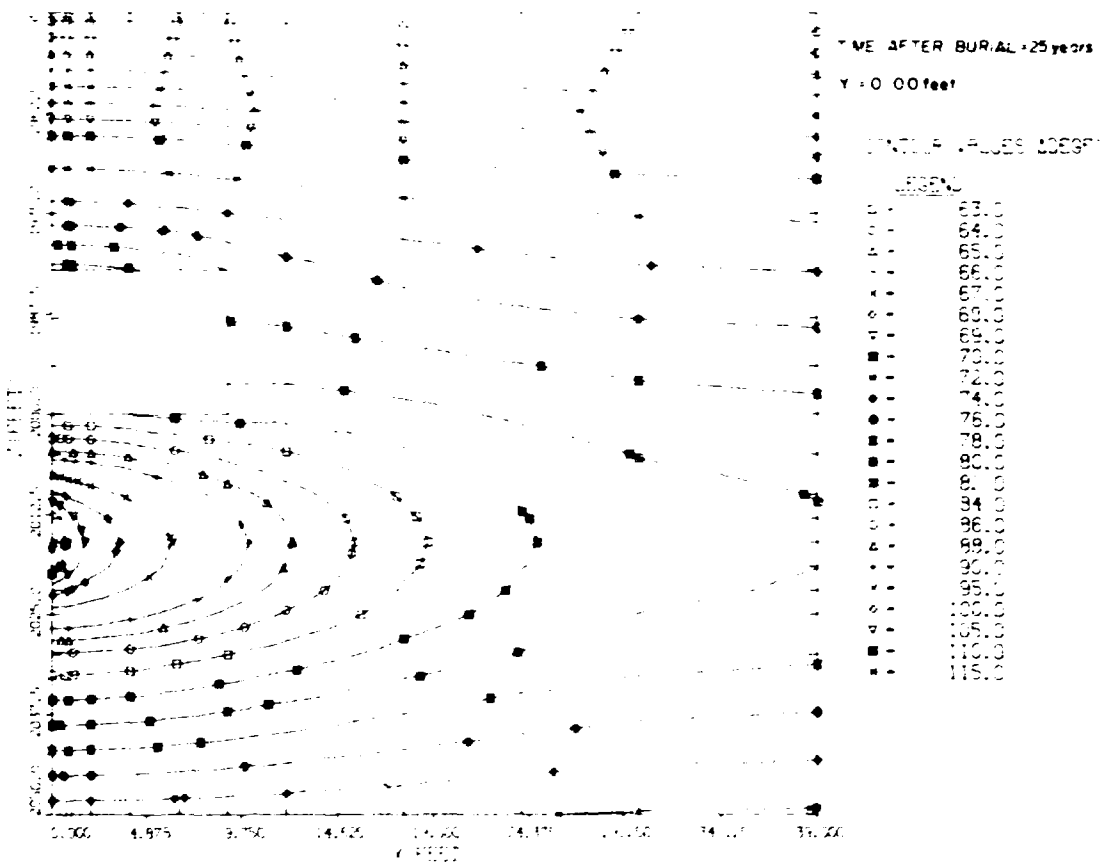

Fig. 8.18. Contours for temperature increases in the *XZ* plane 25 years after burial in the three-dimensional unit-cell model for SF stored at 60 kW/acre.

room 25 years after burial. Notice that ΔT variations up to 14°F are found in the midplane between the canisters that are spaced 5.12 ft apart along the same room, whereas as much as 35°F ΔT variations were noted between the canisters that are spaced in adjacent rooms 78 ft apart.

Similar isotherms have been generated from case 6 for HLW. Figure 8.20 shows the isotherms in the *XZ* plane from case 6 for HLW just prior to scheduled backfilling, 5 years after burial. Figure 8.21 shows isotherms at the midplane, which emphasizes again that the variations in ΔTs occurring between canisters can be as much as 155°F.

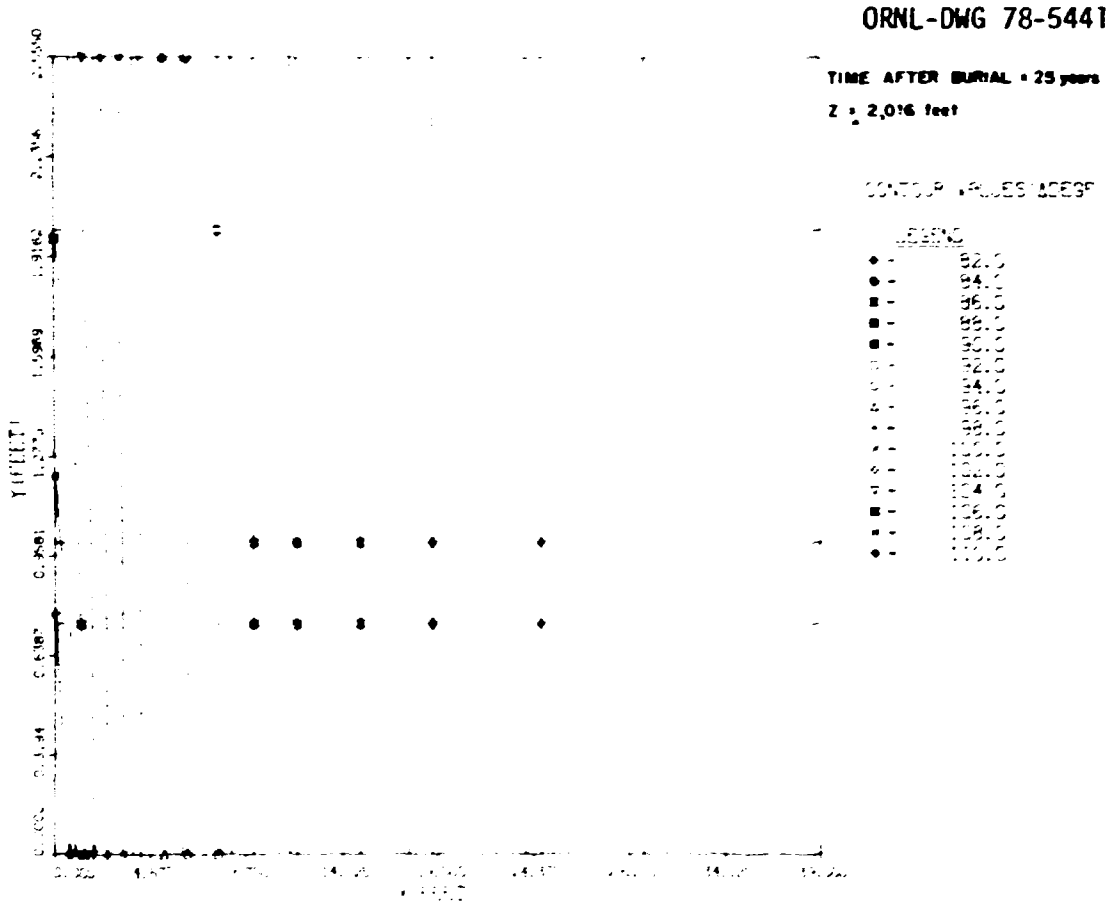

Fig. 8.19. Contours for temperature increases in the horizontal midplane 25 years after burial in the three-dimensional unit-cell model for SF stored at 60 kW/acre.

8.5 Multiple Row Far-Field Model of a High-Level Repository (Case 7) and Numerical Results

The unit-cell models previously described and analyzed have provided a means of calculating conservative maximum temperature increases in the storage media for the terminal and retrievable storage of SF and HLW.

General temperature increases remote from the source are obtained from the far-field models. The actual temperature distribution in the repository will consequently lie somewhere in between and can be predicted only by a complete simulation of the entire repository, which would include both the near-field and far-field effects. Such a model would be very complex, include millions of nodes, and require excessive computer time and storage.

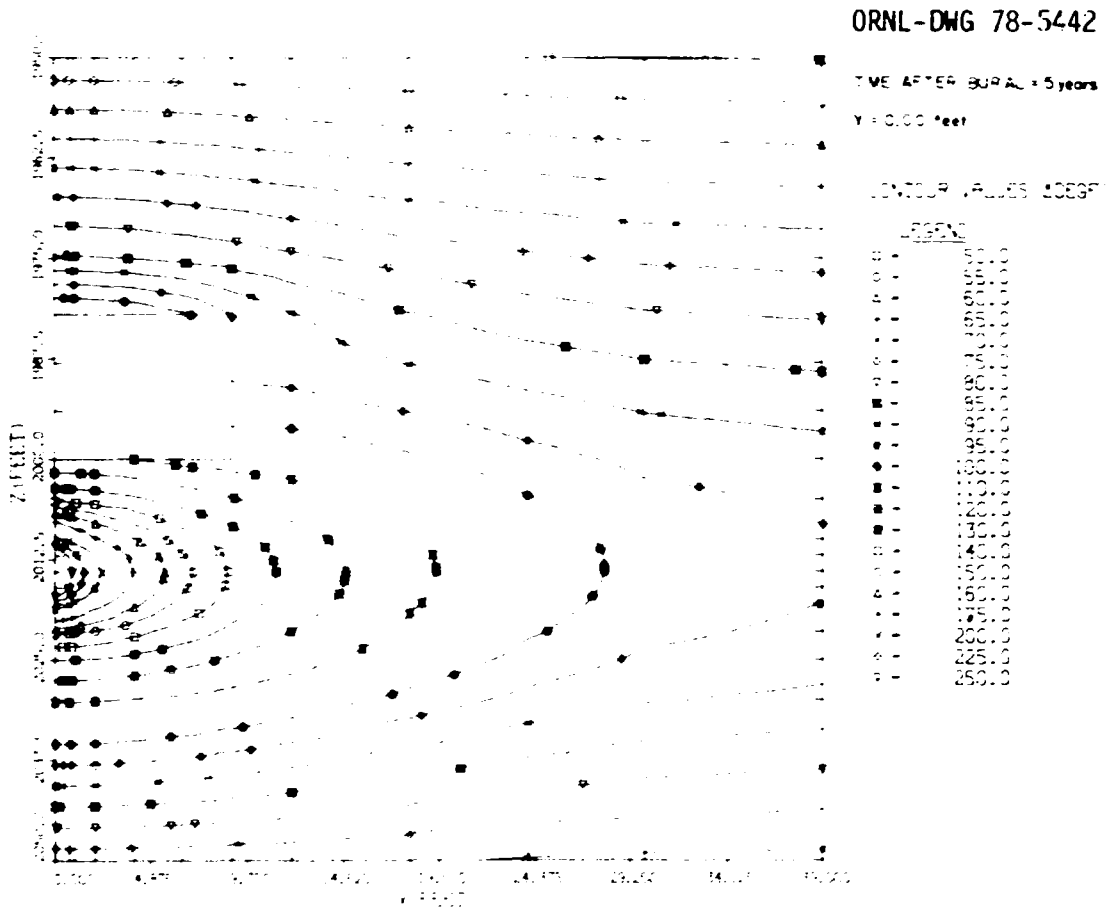

Fig. 8.20. Contours for temperature increases in the *XZ* plane 5 years after burial in the three-dimensional unit-cell model for HLW stored at 150 kW/acre.

As a supportive far-field model, a multiple row, partially homogenized model has been developed which does not simulate each unit cell (canister) by itself but partially takes its effect into account by using multiple rows of infinite slabs in a two-dimensional model. By comparing the two-dimensional far-field homogenized model with the multiple row model, we were able to establish credible temperature limits produced by the far-field homogenized model.

A section through a repository assumed to contain canisters of HLW loaded on infinitely long 1-ft-wide rows spaced 78 ft apart is shown in Fig. 8.22. This configuration models an HLW repository with an initial heat production rate of 150 kW/acre from a depth of 2010 to 2018 ft, as specified in the conceptual repository design. The homogenized heat

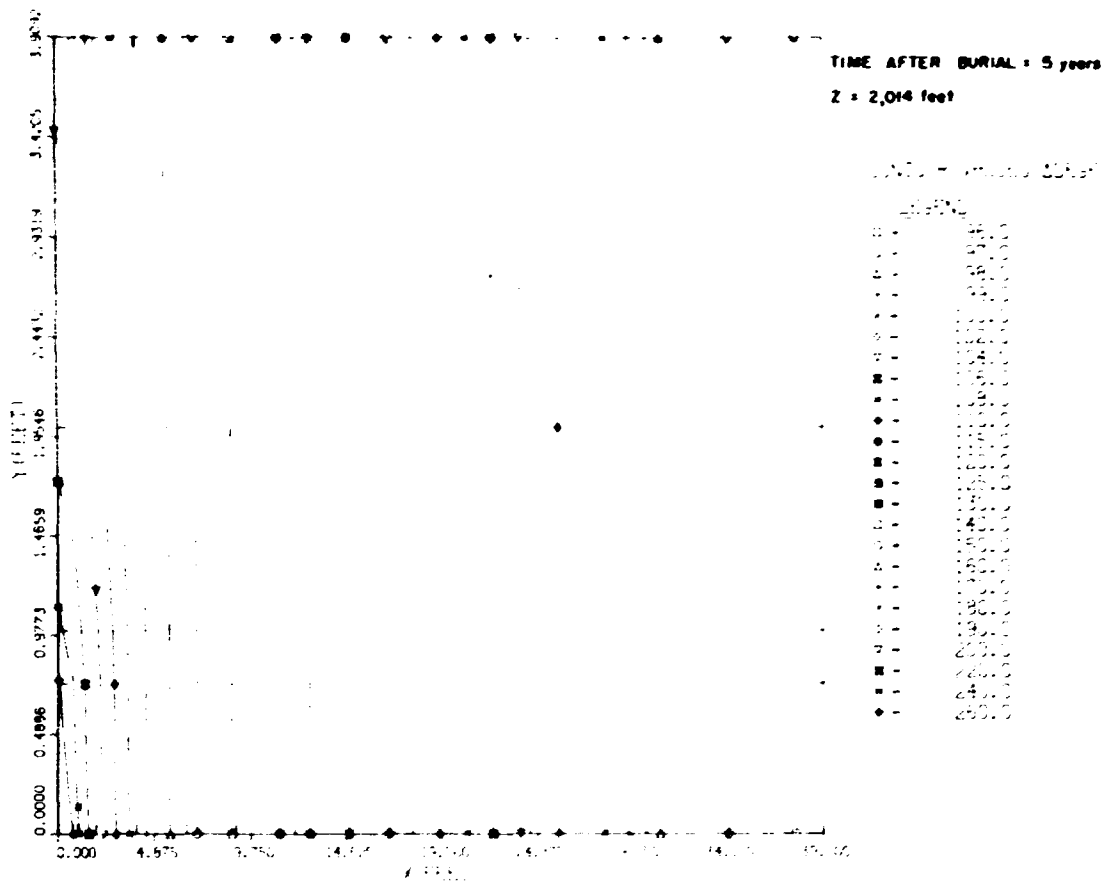

Fig. 8.21. Contours for temperature increases in the horizontal midplane 5 years after burial in the three-dimensional unit-cell model for HLW stored at 150 kW/acre.

generation in each infinite slab is based on 2.1 kW being uniformaly distributed in a slab volume that is 1 ft thick, 8 ft high, and 7.82 ft deep (which is the pitch of the canister emplacement), which yields a volume of 62.55 ft^3 and an initial heat generation rate of 1.0×10^6 $Btu/yr \cdot ft^3$. The actual HLW heat source is about 280 times the strength of the homogenized source used in the two-dimensional, completely homogenized far-field model but only about 3-1/2 times as strong as the partially homogenized source used in the multiple row model.

The modeled repository extends from the center of the repository to 3510 ft, which is 39 ft past the centerline of the last row of canisters.

The axial limits of the model are confined from 880 to 4000 ft, and the *X* direction extends to 4000 ft, which is adequate for the time span

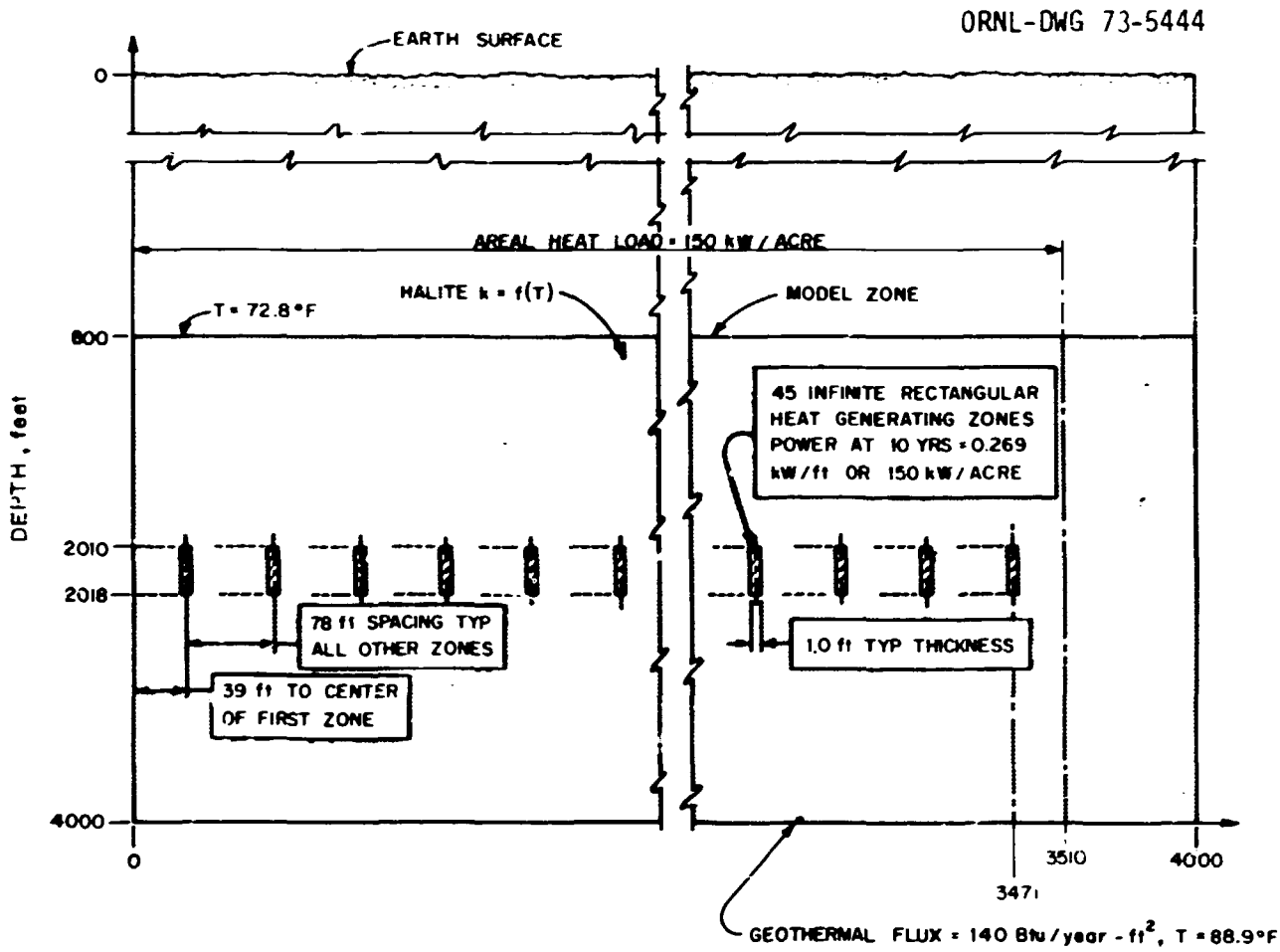

Fig. 8.22. Section through multiple row model showing repository from the center to the edge.

involved. Nodes were selected to obtain temperature distribution between the rows of slabs as well as on their centers. A geothermal flux of 140 Btu/yr·ft^2 was imposed on the lower axial boundary. An initial linear temperature distribution is assumed to range from 72.8°F at 800 ft to 88.9°F at a depth of 4000 ft. The HEATING5A computer program was used to analyze this model.

Figure 8.23 shows the temperature increases at the edge of the repository as functions of the horizontal distance from the center of the repository at various elevations 27 years after burial, the time at which the peak ΔT of this model is reached.

Notice that all of the "peaks" and "valleys" in the ΔTs remain fairly constant as a function of horizontal position throughout the repository.

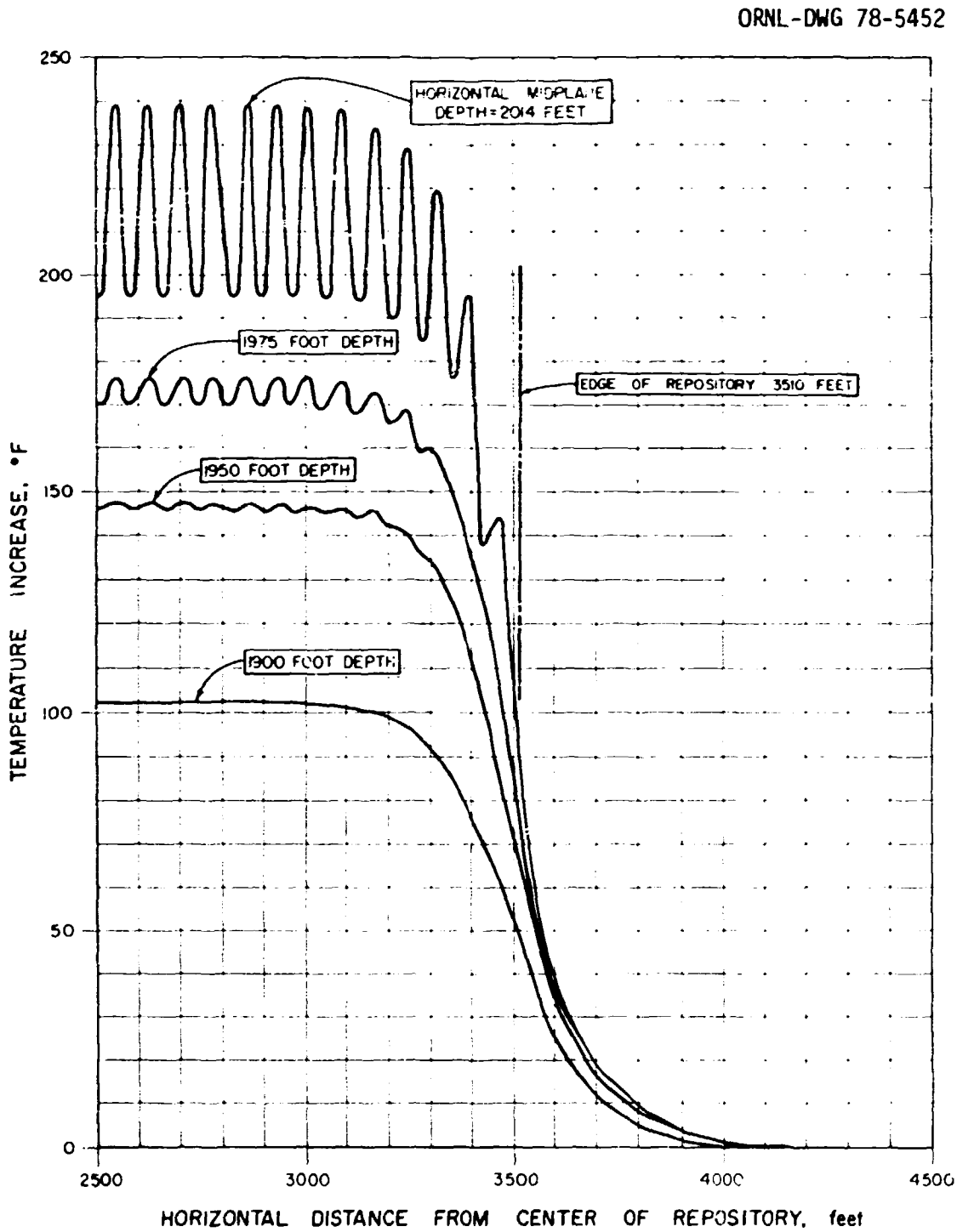

Fig. 8.23. Temperature increases at various depths in the salt repository as a function of horizontal position.

At the horizontal midplane the peak ΔT is about 239°F whereas the ΔT in the valley is about 195°F, which indicates temperature variations as much as 44°F between the rooms. This temperature differential is actually a function of time and was found to be as much as 62°F 1 year after burial, diminishing to as little as 7°F 100 years after burial. The three-dimensional model predicted variations of 170°F 1 year after burial, diminishing to 121°F 20 years after burial. The difference is due to the partial heat source homogenization taking place in the multiple row model.

Figure 8.23 also shows the perturbations (peaks and valleys) in temperature increases at elevations more remote from the source. It is important to note that the perturbations have almost subsided at a depth of 1950 ft and have completely subsided at a depth of 1900 ft. The effect of the temperature perturbations in the radial direction is also confined to within about 100 ft of the edge of the repository.

This observation can serve as an indication that the two-dimensional completely homogenized model is a valid and representative model for zones beyond about 100 ft both horizontally and vertically away from the repository. The multiple row model also gives a better representation of the temperature distribution around the edge of the repository. The peak ΔTs obtained from the analysis of the multiple row model should not be construed as realistic local maximum ΔTs since they are the results of homogenized heat sources; the unit-cell models are to be used for this purpose.

9. COMPARISON OF RESULTS FROM HLW MODELS

In order to ascertain the range of validity of the various models, it was necessary to make comparisons of maximum temperature increases (ΔTs) as functions of both time and position for the models. To simplify the effort, these comparisons are limited to HLW stored at 150 kW/acre and 2.1 kW/canister. Five models are considered in this comparison and include one-dimensional and two-dimensional homogenized far-field models, a two-dimensional partially homogenized model, and both two- and three-dimensional unit-cell models. These models have been described and analyzed in previous sections, but the models and the results have not yet been compared.

The time required for the temperatures or the temperature increases (ΔTs) to peak varies from model to model. The earliest peaking time encountered is in the three-dimensional model, which peaks 20 years after burial; the two-dimensional unit-cell model peaks after 25 years. The two-dimensional multiple row far-field model peaks in 27 years, and the one-dimensional and two-dimensional far-field homgenized models peak last — both in 35 years. These differences are due to concentration of the heat source, the location of the adiabatic boundaries, and the heat capacitance of the model.

Comparisons of ΔTs obtained for HLW from the various models as functions of time and position will be made in the following sections.

9.1 Temperature Differences as Functions of Time

Increases in the midplane salt temperature (ΔTs) from 195 to 301°F were obtained from the various models shown in Fig. 9.1. This plot shows how the maximum salt ΔTs located on the horizontal midplane vary with time. The differences noted over the complete range of all of the models is really not significant because the unit-cell and far-field models are intended for two entirely different purposes. The unit-cell results are for local maximum representation, whereas the far-field models are for average repository representation. These comparisons are necessary, however, to convey to the reader some idea of the divergence of the model types.

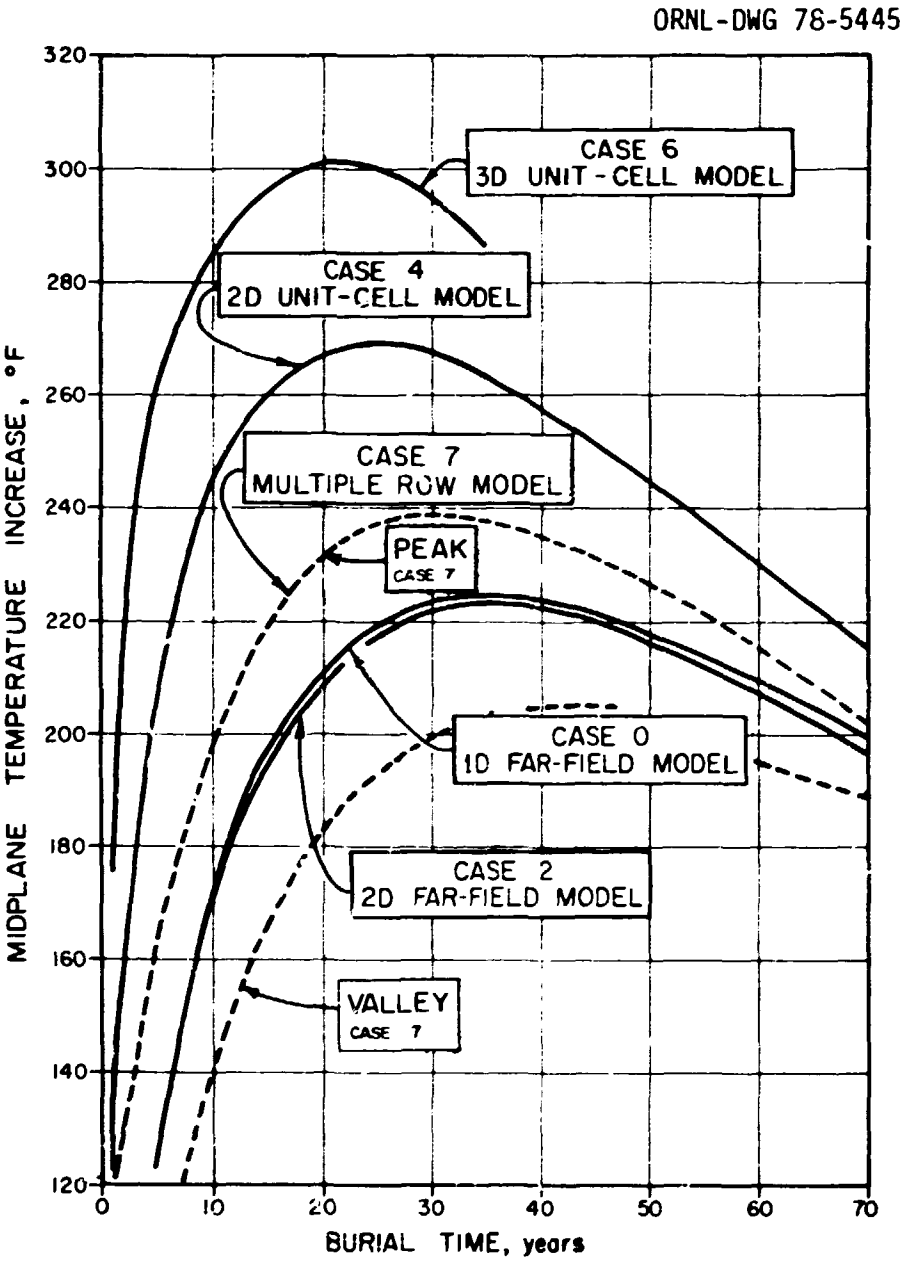

Fig. 9.1. Comparison of temperature increases from various models of a HLW repository as functions of time.

A difference of 32°F or 35% was noted in the ΔTs obtained in the unit-cell models. The marked difference in the unit-cell models is due to difference in the geometrical configuration of the areas of the two models, the location of the adiabatic boundaries, and the fact that the three-dimensional model has an air-filled room, whereas the two-dimensional model

does not consider the room. If the air-filled room in the three-dimensional model were filled with solid salt, the maximum ΔT obtained from both the two-dimensional and three-dimensional unit-cell models would probably be much closer, although differences should still be noted in their distribution because of the difference in geometrical configurations.

The maximum ΔT of 260°F obtained in the salt at the time of backfilling — 5 years after burial — should be the main point of interest for the HLW repository having the assumed stratigraphy and loading used in this study because temperatures developed after backfilling are not of much concern to the designer. The three-dimensional unit-cell model seems to be not only more conservative but also simulates the actual situation quite accurately over most of the repository area. This conclusion is based on the observation from both the two-dimensional homogenized and two-dimensional multiple row far-field models that (1) not much heat flow interchange is taking place between the canisters throughout most of the repository (Figs. 8.6, 8.7, and 8.12) and (2) the three-dimensional unit-cell model exerts the same characteristics of temperature variations between canisters as are also observed in the peaks and valleys of the multiple row model (Fig. 8.23).

In comparing the far-field models, it must be emphasized that the ΔTs shown in Fig. 9.1 do not represent any one point in space but rather temperature increase, which, as indicated before, was found to be fairly uniform throughout most of the repository. In this comparison, it is interesting to note that the peak ΔTs obtained from the one-dimensional and two-dimensional far-field models are in very close agreement. If maximum axial temperature distributions were the only results desired, it would probably be quite satisfactory (at least to within several hundred feet of the source) to use one-dimensional models in making parameter studies. This offers the possibility of quite a saving since the CPU time is only about 4% of that required in the analysis of the two-dimensional homogenized model.

The peaks and valleys of the multiple row model show the temperature fluctuations expected between the rows of canisters, and the average is in agreement with the one-dimensional and two-dimensional homogenized far-field models. These fluctuations are not as steep as those observed in

the three-dimensional unit-cell model because of the partial homogenization of the heat source along each row. The three-dimensional unit-cell results are much more realistic in this respect.

Comparisons of midplane ΔTs obtained at the edge of the HLW repository from two-dimensional far-field models are shown in Fig. 9.2. A peak ΔT of 148°F is produced on the horizontal midplane on the outer row of the repository in the multiple row far-field model 20 years after burial at a distance of 3471 ft from the center of the repository or about 39 ft inside from the edge. This peak on the outer row is reached 7 years before the peak is reached in the center of the repository. A peak ΔT of 89°F is found at the edge of the repository 3510 ft from the center of the multiple row model. This peak is reached 35 years after burial. A peak ΔT of 102°F is observed at the edge of the repository 3500 ft from the center of the horizontal midplane in the two-dimensional homogenized far-field model; this peak is also reached 35 years after burial. It is apparent from these observations that peripheral repository ΔTs on the horizontal midplane require 35 years or more to peak depending on their proximity to the repository, whereas about 20 years are required inside of the repository. The peak ΔTs calculated on the edge of the repository are about 15% greater for the homogenized model than for the partially homogenized multiple row model because heat generation in the homogenized model is extended all the way to the edge. At distances of 100 ft or more from the edge of the repository along the horizontal midplane, the ΔTs from both far-field models are about the same.

It appears that the two-dimensional homogenized far-field model is conservative on the edge and becomes valid at distances of 100 ft or greater from the repository zone.

The peak repository midplane temperature increases expected from the far-field analysis are shown in Fig. 9.3 as functions of areal power for both SF and HLW. These are approximate values taken from the models analyzed in this study (as indicated) and from the results presented in ref. 1. The height referred to in the figure is the height of the homogenized heat generation zone in the two-dimensional far-field model based on the active height of the heat production in the canister.

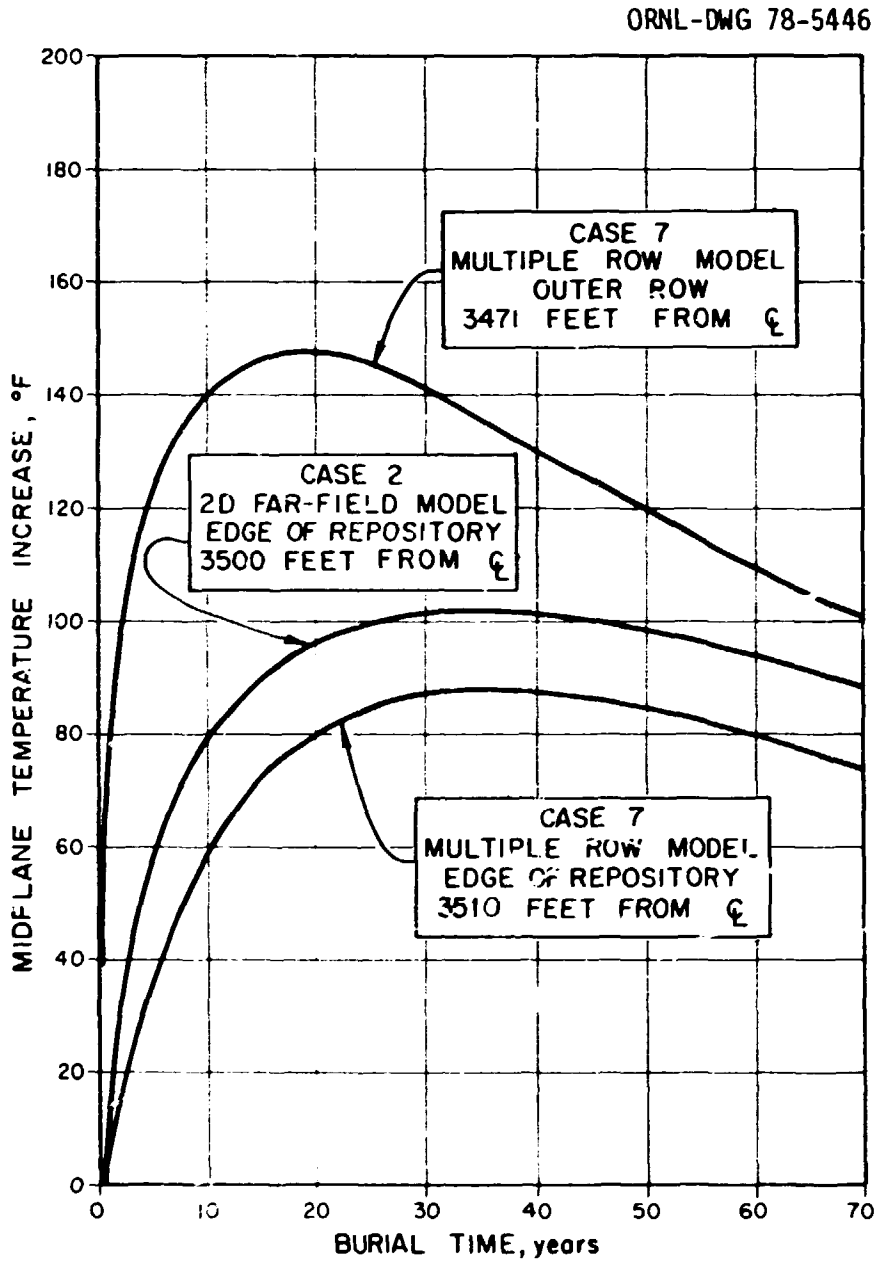

Fig. 9.2. Comparison of midplane temperature increases on outer edge of repository obtained from two-dimensional far-field models storing HLW at 150 kW/acre as functions of time.

9.2 Peak Temperature Increases as Functions of Depth Below the Surface of the Earth

Peak ΔTs as functions of depth below the surface of the earth are shown in Fig. 9.4 for various far-field models at the time the peaking in each model occurs. Notice that within the 100-ft distance above and below

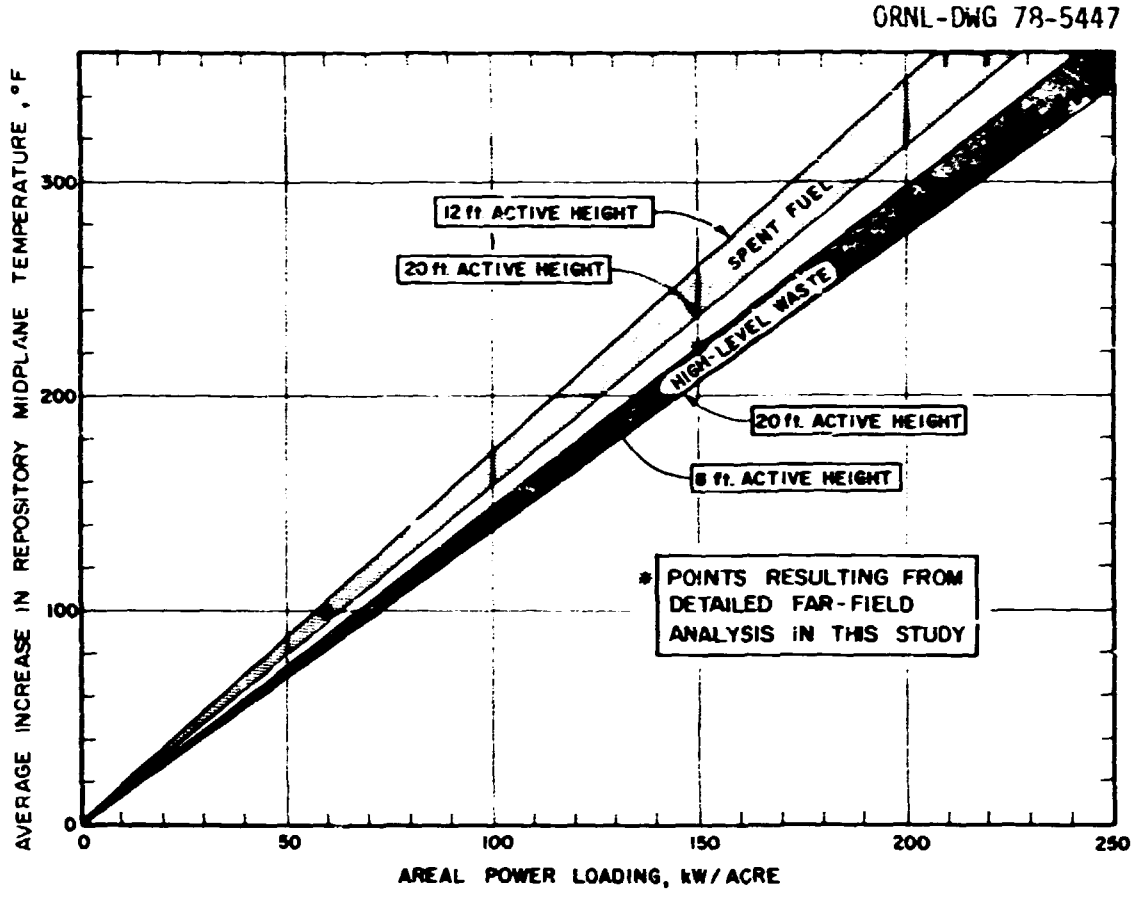

Fig. 9.3. Midplane temperature increases in far-field models produced by SF and HLW as a function of areal heat load.

the midplane, the differences between peaks and valleys in the partially homogenized multiple row model are apparent, but when averaged, the ΔTs are in close agreement with the completely homogenized two-dimensional model. Beyond the 100-ft distance, the perturbations subside completely, and the homogenized models can be considered as realistic representation of the temperatures expected.

Figure 9.5 shows the comparison of peak ΔTs obtained from two-dimensional and three-dimensional unit-cell models as functions of depth below the earth's surface. As previously mentioned, the three-dimensional model assumes a rectangular nonbackfilled room, which reduces the heat capacitance and conductance of the three-dimesnional model and places the heat source much closer to the adiabatic boundary. These conditions contribute to the earlier peaking at the central location on the horizontal midplane

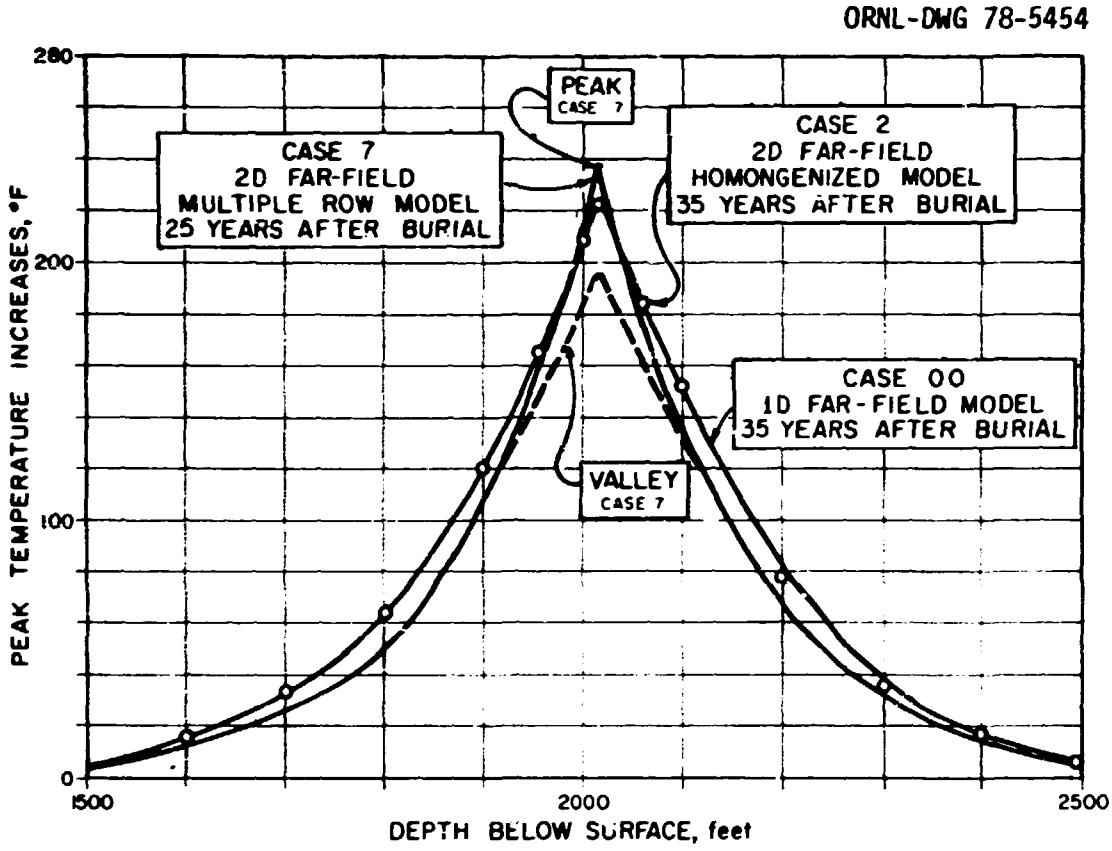

Fig. 9.4. Comparison of peak temperature increases obtained from various far-field models for storing HLW as functions of depth below the surface of the earth.

in the three-dimensional model as compared with the two-dimensional model. The sealed air-filled room also adds resistance to heat flow and increases the peak maximum ΔT in the salt.

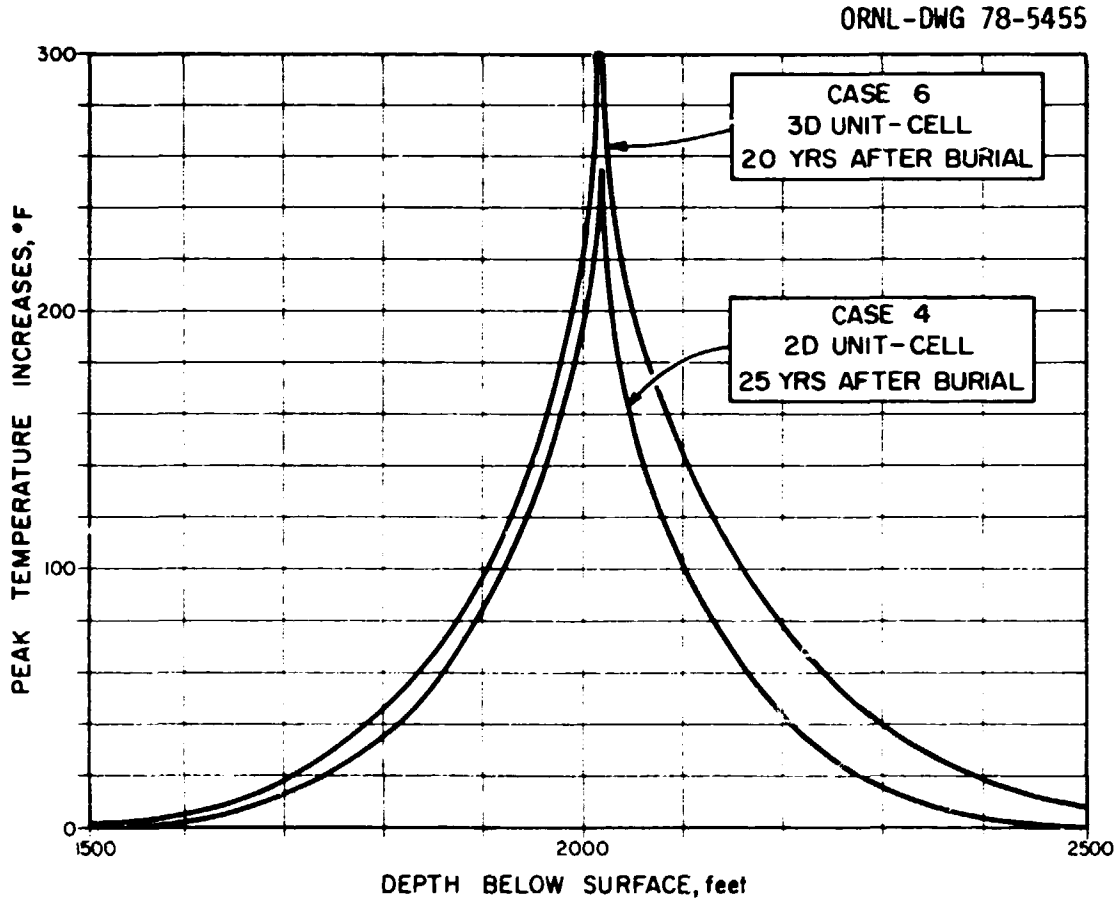

Fig. 9.5. Comparison of peak temperature increases from two- and three-dimensional unit-cell models as functions of depth below the surface of the earth, incurred in the storage of HLW at 150 kW/acre.

10. RESULTS AND CONCLUSIONS

A study has been made of the temperature distribution that results within and outside a repository storing either SF or HLW. First, preliminary simulations of far-field and unit-cell configurations have been made for both cases with an areal heat load of 150 kW/acre. The main conclusion from this part of the analysis is that, for the same areal power distribution (150 kW/acre), the maximum temperature increase for SF is about 19% higher than for HLW based on far-field analysis and 12% based on unit-cell analysis.

From thermoelastic analysis, it was found that a comparable upheaval of the earth is expected from storing either SF with areal power distribution of 60 kW/acre or HLW with areal power distribution of 150 kW/acre. Far-field and unit-cell analyses have been performed for those cases with the following results and conclusions.

1. The maximum ΔT expected in an open repository containing 10-year-old HLW stored at 150 kW/acre and 2.1 kW/canister under the assumption outlined in this report is about 260°F, which results in a maximum temperature of about 339°F occurring prior to backfilling (5 years after burial). The anticipated maximum temperature rise in the floor 5 years after burial in a sealed, but not backfilled, room is about 210°F, which results in accessible temperatures of about 289°F.

2. The maximum ΔT expected in an open repository containing SF stored 60 kW/canister prior to backfilling (25 years after burial) is about 105°F, which results in a maximum temperature of 184°F. In the case of the SF, the peak ΔT on the floor of the room prior to backfilling (25 years after burial) is about 82°F, producing accessible temperatures of about 161°F.

3. Ground surface ΔTs of no more than 0.01°F are expected directly over a repository initially containing 133 MW of either SF or HLW buried in a salt repository at a depth of 2000 ft.

4. The HLW produces a maximum peak ΔT about three times that of the SF but requires only 40% of the storage area and 25% of the number of canisters, but the anticipated thermal uplift is about the same. After about 300 years, the peak ΔTs in the SF exceed those in the HLW.

The following conclusions were made after comparing the results of the various models.

1. The far-field models have shown that radial heat flow within the repository is negligible, which reinforces the assumption of adiabatic boundary conditions on the unit-cell models over most of the repository area.

2. The ΔTs produced by the homogenized far-field models are valid at distances greater than 100 ft from the homogenized heat source based on comparisons made with the multiple row model, which more accurately simulates the edge of the repository.

3. There is an appreciable variation in horizontal midplane temperatures between the canisters as noted from the three-dimensional unit-cell model and substantiated by the multiple row far-field model.

4. The unit-cell models predict conservative peak maximum salt temperature increase which are representative not only at the repository center but over about 80% of the total repository area.

5. The three far-field models yield results that support each other. The one-dimensional model is the least expensive and the most convenient to use when only temperature distribution versus depth is desired.

6. The three-dimensional unit-cell model seems to be conservative, but not overly so. It simulates both the heat sources and the geometry in the most realistic way and supports the adiabatic boundary assumption that was substantiated with the far-field models for most of the repository area. This model seems to be most useful for both peak maximum temperature prediction as well as for estimating temperature variations between the canisters and in the open rooms.

References

1. G. D. Callahan and J. L. Ratigan, *Thermoelastic Analysis of Spent Fuel Repositories in Bedded and Dome Salt*, Y/OWI/SUB-77/22303/4, RE/SPEC, Inc., Rapid City, S.D., 1977.

2. R. D. Cheverton and W. D. Turner, *Thermal Analysis of the National Radioactive Waste Repository: Progress through March 1972*, ORNL-4789, Oak Ridge National Laboratory, September 1972, p. 29.

3. C. W. Kee, A. G. Croff, and J. O. Blomeke, *Updated Projections of Radioactive Wastes to be Generated by the U.S. Nuclear Power Industry*, ORNL/TM-5427, Oak Ridge National Laboratory, December 1976, p. 30.

4. R. D. Cheverton and W. D. Turner, *Thermal Analysis of the National Radioactive Waste Repository: Progress through March 1972*, ORNL-4789, Oak Ridge National Laboratory, September 1972, p. 54.

5. H. S. Carslaw and J. C. Jaeger, *Conduction of Heat in Solids*, Oxford University Press, 1959, Chap. 2.

6. L. R. Ingersoll, O. J. Zobel, and A. C. Ingersoll, *Heat Conduction With Engineering, Geological and Other Applications*, University of Wisconsin Press, 1954, p. 143.

7. J. P. Nichols, Oak Ridge National Laboratory, personal communication to G. H. Llewellyn, March 1971.

8. A. L. Edwards, *TRUMP: A Computer Program for Transient and Steady-State Temperature Distributions in Multidimensional Systems*, revision 3, UCRL-14754, Lawrence Livermore Laboratory, Sept. 1, 1972.

9. R. G. Lawton, *The AYER Heat Conduction Computer Program*, LA-1513-MS, Los Alamos Scientific Laboratory, May 1974.

10. I. Farhoomand and E. L. Wilson, *Nonlinear Heat Transfer of Axisymetric Solids*, Structural Engineering Laboratory, University of California, Berkeley, Calif., April 1971.

11. W. D. Turner, D. C. Elrod, and I. I. Siman-Tov, *HEATING8 — An IBM 360 Heat Conduction Program*, ORNL/CSD/TM-15, Oak Ridge National Laboratory, March 1977.

12. B. C. Kaplan, D. B. Mitchell, and A. H. Moore, "A Comparison of the Crandall and Crank-Nicholson Methods for Solving a Transient Heat Conduction Problem," *Int. J. Numer. Methods Eng.* 9(4): 938-43 (1975).

13. R. D. Cheverton and W. D. Turner, *Thermal Analysis of the National Radioactive Waste Repository: Progress through June 1971*, ORNL-4726, Oak Ridge National Laboratory, p. 4.

14. G. W. Giles, *"HEATING8A,"* letter to D. W. Turner, Dec. 5, 1977.

15. D. W. Turner and D. C. Elrod, letter to R. H. Odegaarden. Office of Nuclear Material Safety and Safeguard, May 12, 1972.

16. C. W. Kee, A. G. Croff, and J. O. Blomeke, *Updated Projections of Radioactive Wastes to be Generated by the U.S. Nuclear Power Industry*, ORNL/TM-5427, Oak Ridge National Laboratory, December 1976, p. 33.

17. R. D. Cheverton and W. D. Turner, *Thermal Analysis of the National Radioactive Waste Repository: Progress through March 1972*, ORNL-4789, Oak Ridge National Laboratory, September 1972, p. 78.

18. M. J. Bell, *ORIGEN — The ORNL Isotope Generation and Depletion Code*, ORNL-4628, Oak Ridge National Laboratory, May 1973.

19. G. D. Smith et al., *Soil-Temperature Regimes, Their Characteristics and Predictability*, SCS-Tp-144, USDA Soil Conservation Service, April 1964.

20. T. Kusuda, National Bureau of Standards, U.S. Department of Commerce, Gaithersburg, Md., personal communication.

21. E. C. Robertson, *The Nature of the Solid Earth*, McGraw-Hill, Inc., 1972, Chap. 19.

22. B. Gutenberg, *Physics of the Earth Interior*, Academic Press, New York, 1959, p. 130.

23. R. D. Cheverton and W. D. Turner, *Thermal Analysis of the National Radioactive Waste Repository: Progress through March 1972*, ORNL-4789, Oak Ridge National Laboratory, September 1972, pp. 33-34.

24. F. Birch and H. Clarke, "The Thermal Conductivity of Rocks and Its Dependence Upon Temperature and Composition," Part II, *Am. J. Sci*, 238613-35 (1940).

25. D. D. Smith, *Thermal Conductivity of Halite Using a Pulsed Laser*, Y/DA-7013, Oak Ridge Y-12 Plant, Dec. 13, 1976.

26. B. Gutenberg, *Physics of the Earth Interior*, Academic Press, New York, 1959, p. 124.

27. A. M. Jessop, M. A. Hobart, and J. G. Sclater, *The World Heat Flow Data Collection — 1975*, Geothermal Service of Canada, Geothermal Series No. 5, Ottawa, Canada, 1976.

28. R. D. Cheverton and W. D. Turner, *Thermal Analysis of the National Radioactive Waste Repository: Progress through March 1972*, ORNL-4789, Oak Ridge National Laboratory, September 1972, p. 1.

29. T. G. Godfrey, S. H. Jury, D. L. McElroy, *Radioactive Waste Repository Project; Annual Progress Report, Period Ending Sept. 30, 1972*, ORNL-4824, Oak Ridge National Laboratory, p. 218.

30. D. C. Elrod and W. D. Turner, *HEATPLOT — A Temperature Distribution Plotting Program for HEATING5*, K/CDS/TM-11, Oak Ridge K-25 Plant, July 1977.